Palaeogeography, Palaeoclimatology, Palaeoecology 410 (2014) 164–178

Contents lists available at ScienceDirect

Palaeogeography, Palaeoclimatology, Palaeoecology

journal homepage: www.elsevier.com/locate/palaeo

Linking Holocene drying trends from Lonar Lake in monsoonal central India to North Atlantic cooling events

Philip Menzel [a,*], Birgit Gaye [a], Praveen K. Mishra [b], Ambili Anoop [b,1], Nathani Basavaiah [c], Norbert Marwan [d], Birgit Plessen [b], Sushma Prasad [e], Nils Riedel [f], Martina Stebich [f], Martin G. Wiesner [a]

[a] Institute of Geology, University of Hamburg, Bundesstr. 55, 20146 Hamburg, Germany
[b] Helmholtz-Centre Potsdam, German Research Centre for Geosciences (GFZ), Telegrafenberg, 14473 Potsdam, Germany
[c] Indian Institute of Geomagnetism, Plot 5, Sector 18, New Panvel, Navi Mumbai 410218, India
[d] Potsdam-Institute for Climate Impact Research, Telegrafenberg A 51, 14412 Potsdam, Germany
[e] Institute of Earth- and Environmental Science, University of Potsdam, Karl-Liebknecht-Str. 24-25, 14476 Potsdam-Golm, Germany
[f] Senckenberg Research Station of Quaternary Palaeontology, Am Jakobskirchhof 4, 99423 Weimar, Germany

ARTICLE INFO

Article history:
Received 27 November 2013
Received in revised form 22 May 2014
Accepted 30 May 2014
Available online 10 June 2014

Keywords:
Lake sediment
Indian monsoon
Holocene
Climate reconstruction
Stable carbon isotope
Amino acid

ABSTRACT

We present the results of biogeochemical and mineralogical analyses on a sediment core that covers the Holocene sedimentation history of the climatically sensitive, closed, saline, and alkaline Lonar Lake in the core monsoon zone in central India. We compare our results of C/N ratios, stable carbon and nitrogen isotopes, grain-size, as well as amino acid derived degradation proxies with climatically sensitive proxies of other records from South Asia and the North Atlantic region. The comparison reveals some more or less contemporaneous climate shifts. At Lonar Lake, a general long term climate transition from wet conditions during the early Holocene to drier conditions during the late Holocene, delineating the insolation curve, can be reconstructed. In addition to the previously identified periods of prolonged drought during 4.6–3.9 and 2.0–0.6 cal ka that have been attributed to temperature changes in the Indo Pacific Warm Pool, several additional phases of shorter term climate alteration superimposed upon the general climate trend can be identified. These correlate with cold phases in the North Atlantic region. The most pronounced climate deteriorations indicated by our data occurred during 6.2–5.2, 4.6–3.9, and 2.0–0.6 cal ka BP. The strong dry phase between 4.6 and 3.9 cal ka BP at Lonar Lake corroborates the hypothesis that severe climate deterioration contributed to the decline of the Indus Civilisation about 3.9 ka BP.

1. Introduction

The increasing demand for reliable climate projections due to the challenges related to global warming calls for enhanced investigation of the relationship between climate change and its effect on the environment. To assess future interaction between climate and environment, it is necessary to understand their interactions in the present and past. But, while modern observations are increasing rapidly and cover almost the whole world in high spatial and temporal resolution, the identification and investigation of suitable sites for palaeoclimate reconstruction is more difficult and requires great effort. Hence, several regions still lack a sufficient cover of investigated areas to help the scientific community in reconstructing the past climate and its influence on the former environment. One of these regions is India, which highly depends on the annual rainfall delivered by the Indian summer monsoon (ISM). This meteorological phenomenon affects a human population of more than one billion and is highly sensitive to climate change. In order to assess and to interpret potential future modifications of the Indian monsoon system, the knowledge of Holocene monsoon variability, its extremes, and their underlying causal mechanisms is crucial. And while terrestrial palaeorecords are available from the northern Indian subcontinent and the Himalayan region (Gasse et al., 1991, 1996; Enzel et al., 1999; Denniston et al., 2000; Thompson et al., 2000; Bookhagen et al., 2005; Prasad and Enzel, 2006; Clift et al., 2008; Demske et al., 2009; Wünnemann et al., 2010; Alizai et al., 2012), the number and length of comparable records from central and south India are limited (Yadava and Ramesh, 2005; Caner et al., 2007; Sinha et al., 2007; Berkelhammer et al., 2010). To address this issue, we have investigated the Holocene sedimentation history of Lonar Lake from central India with a special focus on centennial scale palaeoclimate reconstruction.

Based on mineralogical, palynological, and biogeochemical investigations on the ca. 10 m long sediment core, the longest, well dated palaeo-climate archive from India's core monsoon zone, S. Prasad et al.

* Corresponding author. Tel.: +49 40 42838 8288.
E-mail addresses: philip.menzel@zmaw.de (P. Menzel), birgit.gaye@zmaw.de (B. Gaye), mishra@gfz-potsdam.de (P.K. Mishra), anoop@gfz-potsdam.de (A. Anoop), bas@iigs.iigm.res.in (N. Basavaiah), marwan@pik-potsdam.de (N. Marwan), birgit.plessen@gfz-potsdam.de (B. Plessen), sushma.prasad@geo.uni-potsdam.de (S. Prasad), nils.riedel@senckenberg.de (N. Riedel), martina.stebich@senckenberg.de (M. Stebich), martin.wiesner@zmaw.de (M.G. Wiesner).
[1] Present address: Department of Earth Sciences, Indian Institute of Science Education and Research, Kolkata 741252, India.

http://dx.doi.org/10.1016/j.palaeo.2014.05.044
0031-0182/

(2014) reconstructed the broad, Holocene climatic development of the Lonar Lake region, identified two millennial scale dry phases, and discussed the stability of the ISM–El Niño Southern Oscillation (ENSO) links and the influence of shifts in the position of the Indo Pacific Warm Pool (IPWP) on the prolonged droughts in the ISM realm. Here we present stable carbon and nitrogen isotope data from S. Prasad et al. (2014) as well as new data from amino acid, sediment composition, and grain-size analysis and interpret them with respect to centennial scale, Holocene climate variability and its tele-connections with the North Atlantic climate.

Bond et al. (2001) hypothesised a connection between North Atlantic cooling events and cosmogenic nuclide production rates, the latter indicating small changes in solar output. Additionally, they found virtually synchronous "quasi-periodic" ~1500 year cyclicity in both their palaeorecord and nuclide production rates. Thus, they postulated a reaction of climate to small changes in solar output, which would not be limited to the North Atlantic region but which would affect the global climate system (Bond et al., 2001). Correlations between the high and the mid latitude climate, as reconstructed from Greenland ice cores (Stuiver and Grootes, 2000; Johnsen et al., 2001) and ice-rafted debris in North Atlantic deep sea records (Bond et al., 1997), and the low latitude tropical climate have been found in various climate reconstructions (Haug et al., 2001; Gupta et al., 2003; Hong et al., 2003; Dykoski et al., 2005; Wang et al., 2005; Fleitmann et al., 2007; Koutavas and Sachs, 2008) supporting the assumption that different climate systems react to the same cause, like solar output variation (Bond et al., 2001; Soon et al., 2014) either independently or via tele-connections. However, since many palaeoclimate investigations concerning the correlations between tropical climate and North Atlantic climate were carried out in peripheral ISM regions (Hong et al., 2003; Fleitmann et al., 2007), these records could not indicate if the change in moisture availability was exclusively linked to an alteration in monsoonal summer rainfall rather than to altered winter westerly precipitation. Lonar Lake is one of the very few natural lakes located in the core monsoon zone in central India, and it is fed exclusively by precipitation of the Indian summer monsoon and stream inflow that is closely linked to monsoon rainfall (Anoop et al., 2013b). Additionally, available precipitation data from the region close to Lonar Lake indicate a good correlation with the all India rainfall record of the last century (1901–2002). Correlation between the all India rainfall record (ftp://www.tropmet.res.in/pub/data/rain/iitm-regionrf.txt) and the annual precipitation data of the meteorological stations in Buldhana, Jalna, Hingoli, and Washim (http://www.indiawaterportal.org/met_data/) varies between 0.62 and 0.69 ($p < 0.001$), making Lonar Lake a key site to investigate the connection between Indian monsoon strength and its connection to North Atlantic climate change.

2. Study site

Lonar Lake is a closed basin lake situated at the floor of a meteorite impact crater that formed during the Pleistocene (~570 ± 47 ka) on the Deccan Plateau basalts (Jourdan et al., 2011). The lake is located at Buldhana District in Maharashtra, central India at 19.98° N and 76.51° E (Fig. 1). The meteorite crater has a diameter of ca. 1880 m, and the almost circular lake covers an area of about 1 km^2. The modern crater floor is located at ca. 470 m above sea level, which is around 140 m below the rim crest elevation. The inner rim wall is fairly steep with slopes of 15–18° in the east and up to ~30° in the west and southwest (Basavaiah et al., 2014).

Lonar Lake is located in the 'core monsoon zone' of the Indian summer monsoon (Gadgil, 2003). The southwest monsoon from June to end of September is characterised by strong winds and brings in average rainfall of ~700 mm. Precipitation during December to April occurs only in rare cases. The temperature can exceed 40 °C before the onset of the monsoon and declines during the monsoon phase to an average of approximately 27 °C. The post monsoon from October to February is characterised by relatively low temperatures at an average of 23 °C

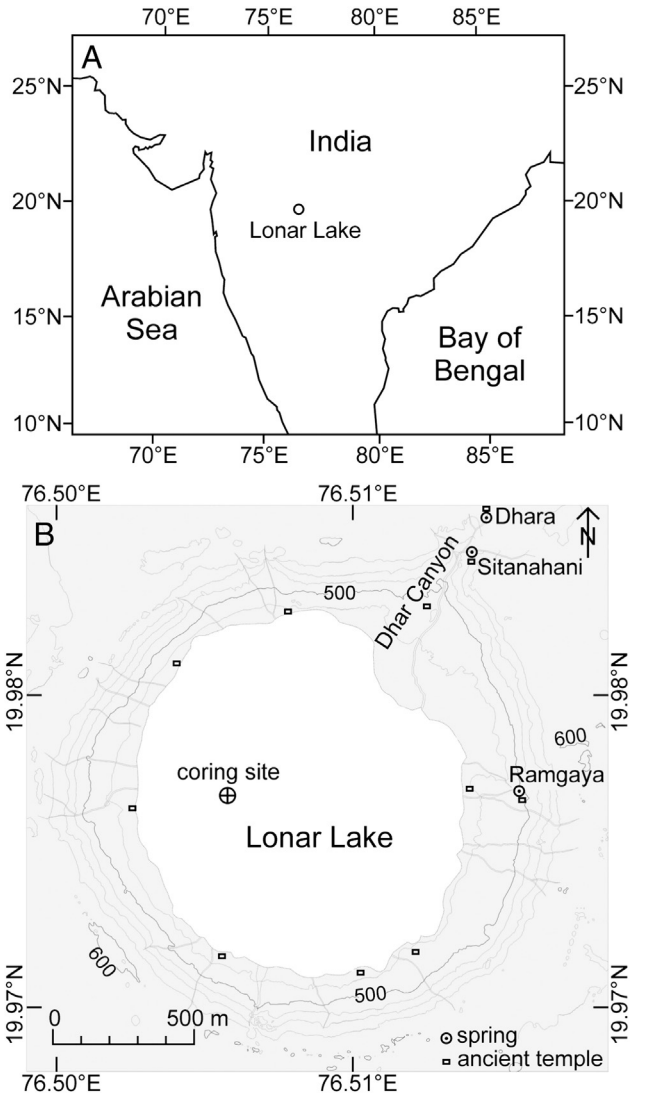

Fig. 1. A: Regional overview and location of Lonar Lake. B: Study area showing the coring site.

(http://indiawaterportal.org/met_data/). The lake is fed by surface runoff during the monsoon season and three perennial streams that are closely linked to monsoon rainfall as indicated by tritium dating (Anoop et al., 2013b). Two of them, the Dhara stream and the Sitanahani stream are entering the crater from the northeast. They have formed the Dhara Canyon, an erosive incision, and have built up an alluvial fan into the lake. Today this fan is used for agricultural plantation. The Ramgaya stream, the third stream feeding the lake, springs from the inner crater wall and enters the lake from the eastern shore. Nowadays the three streams are diverted towards the Dhara fan to irrigate the agricultural fields. Water discharge is only conducted by evapotranspiration; no outflowing stream is present and no loss due to seepage occurs as the lake level is below the local groundwater level (Nandy and Deo, 1961).

The modern lake is ca. 6 m deep, brackish, alkaline, and eutrophic with permanent bottom water anoxia (Basavaiah et al., 2014). The eutrophication promotes phytoplankton blooms especially during and subsequent to the monsoon when nutrients are washed into the lake. The algal assemblage is primarily made up of cyanophyceae (Badve et al., 1993). Thermophilic, halophilic, and alkalophilic bacteria in numbers of 10^2 to 10^4 viable cells/ml (Joshi et al., 2008) and methanogenic archaea (Surakasi et al., 2007) were reported from Lonar Lake. The lake lacks most zooplankton species and higher organisms. The zooplankton community within the lake consists of ciliates, culicid larvae, and rotifers (Mahajan, 2005). Only few exemplars of the ostracod *Cypris*

subglobosa and the gastropod *Lymnea acuminate* have been observed in the lake (Badve et al., 1993).

The vegetation of the inner crater walls changes from the upper part near the rim crest to the bottom part close to the lake shore. The upper part of the inner crater walls is covered by drought tolerant grass and thorn shrub species, further down grows teak (*Tectona grandis*) dominated dry deciduous forest, and the bottom part of the inner crater walls is overgrown by semi evergreen forests. The alluvial fan, which has formed due to riverine erosion in the northeast of the lake, is used for crop plantation and cattle grazing. The fan is characterised by vegetation cover of grasses, sedges, and crop plants like banana (*Musa* x *paradisiaca*), millet (*Setaria italica*), corn (*Zea mays*), custard-apple (*Annona reticulata*), and papaya (*Carica papaya*) (Menzel et al., 2013).

3. Methods and material

3.1. Sampling

Two parallel ca. 10 m long cores were retrieved in May–June 2008 at 5.4 m water depth using a UWITEC sediment piston corer. The cores were opened in the laboratory; a composite core was constructed and sub-sampled in 0.5 cm resolution using L-channel sampling procedure. All samples except those for grain-size analyses were freeze-dried and ground manually in an agate mortar.

3.2. Analytical methods

The total carbon (TC), total nitrogen (TN), and total organic carbon (TOC) contents and the $\delta^{15}N$ and $\delta^{13}C_{org}$ isotopic composition were determined using an elemental analyser (NC2500 Carlo Erba) coupled with a ConFlowIII interface on a DELTAplusXL mass spectrometer (ThemoFisher Scientific). The isotopic composition is given in the delta (δ) notation indicating the difference, in per mil (‰), between the isotopic ratios of the sample relative to an international standard: $\delta\ (‰) = [(R_{sample} / R_{standard}) - 1] \times 1000$. The ratio and standard for carbon is $^{13}C/^{12}C$ and VPDB (Vienna PeeDee Belemnite) and for nitrogen $^{15}N/^{14}N$ and air N_2, respectively.

For TC, TN and $\delta^{15}N$ determination, around 20 mg of sample material was loaded in tin capsules and burned in the elemental analyser. The TC and TN contents were calibrated against acetanilide whereas for the nitrogen isotopic composition two ammonium sulphate standards (e.g. IAEA N-1 and N-2) were used. The results were proofed with an internal soil reference sample (Boden3). Replicate measurements resulted in a standard deviation better than 0.1% for N and 0.2‰ for $\delta^{15}N$.

The TOC contents and $\delta^{13}C_{org}$ values were determined on in situ decalcified samples. Around 3 mg of sample material was weighted into Ag-capsules, dropped with 20% HCl, heated for 3 h at 75 °C, and finally wrapped into the Ag-capsules and measured as described above. The calibration was performed using elemental (urea) and certified isotopic standards (USGS24, IAEA CH-7) and proofed with an internal soil reference sample (Boden3). The reproducibility for replicate analyses is 0.1% for TOC and 0.2‰ for $\delta^{13}C_{org}$.

Inorganic carbon (IC) was defined as the difference between TC and TOC. IC was converted to carbonate by multiplying with 8.33, since calcium carbonate was the only carbonate phase detected in the sediments despite three distinct zones of the core where gaylussite crystals were found (1.58–4.22 m, 6.42–7.60 m, 9.10–9.25 m). These crystals were handpicked under microscope prior to analyses. Due to negligible contribution of biogenic silica, the percentage of lithogenic material in the sediments was calculated using the formula:

$$\text{Lith}\ (\%) = 100\% - (\text{total organic matter}\ [\%] + \text{carbonate}\ [\%]).$$

Analyses of amino acids (AA) and hexosamines (HA) were carried out on a Biochrom 30 Amino Acid Analyser according to the method described by Lahajnar et al. (2007). Briefly, after hydrolysis of the samples with 6 mol l^{-1} HCl for 22 h at 110 °C under a pure argon atmosphere, HCl was removed from an aliquot by repeated evaporation using a vacuum rotating evaporator (Büchi 011) and subsequent dissolution of the residue in distilled water. After evaporating the aliquot three times, the residue was taken up in an acidic buffer (pH: 2.2) and injected into the analyser. The individual monomers were separated with a cation exchange resin and detected fluorometrically according to the procedure described by Roth and Hampaï (1973). Duplicate analysis of a standard solution according to this method results in a relative error of 0.1 to 1.3% for the concentration of individual AA monomers. Duplicate measurement of a sediment sample revealed a relative error of <1% for AA and HA concentrations, <10% for molar contribution of low concentrated (<1 mol%) AA monomers, and <2.5% for higher concentrated (>1 mol%) AA monomers.

Grain-size distribution of the core samples was determined using a Malvern Mastersizer 2000 analyser. The pre-treatment of sediments included the wet-oxidising of the organic matter and the chemical dissolution of carbonates at room temperature. 0.3 g freeze-dried sample aliquots were treated with 10 ml H_2O_2 (30%) which was added in two steps. The excess oxidising agent was removed by repeated washing with Millipore water (18.2 MΩ cm), centrifugation (6000 rpm, 5 min), and suction of the supernatant. The carbonates of the solid residues were dissolved by the addition of 3.5 ml 1 M HCl over night. The solid residues were repeatedly washed (see above) and suspended in 20 ml Millipore water. The de-acidified samples were kept in an ultrasonic vibrator for 15 min to disaggregate all grains. The instrument measured the grain-size of the suspended particles from 0.02 to 2000 μm for 100 grain-size classes. The content of coarse particles (>200 μm) in the small aliquots exposed to measurement cannot be representative for the entire sample. Therefore, we re-calculated the volume-percentage for the grain-size fraction 0.02 to 200 μm.

3.3. Statistical method

To assess the interrelation of climatic changes in central India and the North Atlantic region as well as the concurrence of climate changes in central India and the solar output we have calculated the major frequencies in our climate proxy data as well as the correlation between our proxy and the ^{14}C production rate. Before the spectral analysis, the long term climate trend was removed from the whole time series by applying a Gaussian kernel based filter with a kernel bandwidth of 500 years. The spectral analysis is then performed as the Fourier transform of the auto-correlation function. Since the sampling of the time series is irregular, the auto-correlation estimation is also based on a Gaussian kernel (bandwidth of 0.5 years), allowing us to directly apply this method without preceding interpolation (Rehfeld et al., 2011). A statistical test was performed to create a confidence interval for the found spectrum. For the test, we have fitted an auto-regressive process of first order (AR1) to the unfiltered original time series, created 10,000 realisations of this AR1 process, and applied the same kernel based high-pass filter as for the original time series. From these 10,000 realisations, we calculated the power spectra by Fourier transform of the auto-correlation function and estimated the 90% confidence interval (software NESToolbox for MATLAB used).

3.4. Chronology

The age model for the core is based on 19 AMS ^{14}C dated samples of wood, leaves, gaylussite crystals, and bulk organic matter (Table 1; S. Prasad et al., 2014). The oldest dated sample of the core shows an age of 11016 ± 161 cal a BP, suggesting that the core covers the complete Holocene sedimentation history of Lonar Lake. The radiocarbon dating was carried out at Poznan radiocarbon laboratory, Poland. Since the catchment geology comprises virtually carbonate free basaltic rocks of the Deccan Traps, no correction for hard water effect was conducted. However, the elevated salinity and pH in combination with

Table 1
Radiocarbon ages from the Lonar Lake core; first published by S. Prasad et al. (2014). Calibration of the ^{14}C dates was carried out using the program OxCal, interpolating with the INTCAL04 and NH3 calibration curves (Bronk Ramsey, 2008).

Lab no.	Material	Composite depth (cm)	^{14}C date (2σ) (^{14}C yr BP)	Calendar age range (2σ) (cal yr BP)
Poz 44133	Bulk	0	116.79 ± 0.84	−55 to −59
Poz 44142	Wood	20	143.51 ± 0.0086	−16 to −28
Poz 44143	Bulk		107.88 ± 0.76	
Poz 27189	Wood	163.5	564 ± 60	669 to 505
Poz 41602	Bulk		760 ± 360	
Poz 41605	Gaylussite crystal	266	1105 ± 60	1076 to 944
Poz 27190	Wood	266.5	1105 ± 60	1079 to 947
Poz 41603	Bulk		1075 ± 60	
Poz 41604	Wood	267.5	1100 ± 60	1086 to 950
Poz 41607	Wood	383.5	1840 ± 70	1924 to 1624
Poz 27236	Wood	482	2315 ± 70	2696 to 2192
Poz 44141	Bulk	511.5	2680 ± 70	2944 to 2580
Poz 44226	Bulk	612	3470 ± 70	3867 to 3531
Poz 27237	Wood	778	4185 ± 70	4911 to 4583
Poz 27191	Wood	820	4600 ± 120	5479 to 4867
Poz 41611	Wood	870	7420 ± 80	8396 to 8096
Poz 27193	Wood	870.5	7460 ± 180	8412 to 8104
Poz 27194	Wood	872	7410 ± 200	8476 to 8100
Poz 27373	Wood	882.5	8880 ± 120	10197 to 9529
Poz 27253	Wood	899	8990 ± 160	10707 to 9867
Poz 27238	Leaf	902	9740 ± 100	11274 to 10670
Poz 27192	Wood	904	9570 ± 200	11338 to 10694

stratification of the water body led to an ageing of the bulk organic matter samples (S. Prasad et al., 2014). Calibration of the ^{14}C dates was carried out using the program OxCal, interpolating with the INTCAL04 and NH3 calibration curves (Bronk Ramsey, 2008).

3.5. Mineralogical and biogeochemical proxies

Our reconstruction of the climatic history of the Lonar Lake region and its comparison to the North Atlantic region is mainly based on lithogenic contribution to the sediments, grain-size, atomic organic carbon to total nitrogen ratio (C/N), $\delta^{13}C_{org}$, $\delta^{15}N$, and amino acid derived indices. The C/N, $\delta^{13}C_{org}$, and $\delta^{15}N$ data were reported and interpreted with respect to climate variability and climatic tele-connections of the Lonar Lake region with the Pacific by S. Prasad et al. (2014). Additionally, the occurrence of evaporitic gaylussite crystals in the sediments, as reported by Anoop et al. (2013b), was used for the climate reconstruction. The mechanisms driving the changes in the parameters are shortly summarised in the following sections.

3.5.1. Lithogenic contribution

The lithogenic contribution to lake sediments mostly depends on the erosion that takes place in the catchment area, transport energy, and shore line proximity (Koinig et al., 2003; Magny et al., 2012). The intensity of erosion at a lake, which is not affected by temperatures below the freezing point, is mostly driven by the amount of rainfall, the occurrence of heavy rainfall events, and the density of vegetation that prevents erosion (Kauppila and Salonen, 1997; Anoop et al., 2013a). Human interferences like deforestation, agricultural land use, and construction activity must be considered as potential causes of enhanced erosion especially in the younger past (Wilmshurst, 1997). Counterintuitively, phases of enhanced precipitation potentially triggering stronger erosion do not necessarily coincide with elevated lithogenic percentages in the lake sediments. This is due to the spreading of vegetation during climatically wet phases, but can also be controlled by changes in lake level. During wet phases, the lake level increases, which also increases the distance between a sampling site and the lake shore. Thus, high proportions of the eroded material from the catchment are deposited relatively close to the shore in shallow water and do not reach the deeper sampling site. These mechanisms seem to dominate at Lonar Lake, since time slices of the Lonar core that show strong evidence of dry climate coincide with high lithogenic contribution to the sediments.

Thus, the lithogenic contribution seems to be a good proxy for the climate reconstruction at Lonar Lake with high values indicating low lake level during drier climate and low values indicating high lake level during wetter climate.

3.5.2. Grain-size

The grain-size of lake sediments depends much on the source of the sediment load. But if the source of the sediments does not change, the grain-size can give information about changes in the hydrodynamics of inflowing streams, the amount of precipitation, the occurrence of heavy rainfall events, seasonality, shore line or sediment source (e.g., river mouth) proximity, changes in the internal hydrodynamics (e.g., currents), and external factors affecting the catchment erosion (McLaren and Bowles, 1985; Sun et al., 2002; Peng et al., 2005). The sorting of the sediments can be used to reconstruct the transport distance and the rate of deposition.

The grain-size data are particularly useful for the broad, Holocene climate reconstruction at Lonar Lake since they depend on changes in monsoon strength. However, for the reconstruction of smaller scale climate variability, the resolution of grain-size data might not be high enough, especially in the lower part of the core, where sedimentation rates are low.

3.5.3. C/N

The C/N ratio is often used to determine the source of organic matter (OM) in lake and coastal sediments (Meyers, 1997). Since aquatic OM is relatively enriched in nitrogen rich proteins, and vascular plant OM is relatively enriched in nitrogen depleted lignin and cellulose, the ratio of carbon to nitrogen is much lower in aquatic OM than in OM of terrestrial origin. C/N ratios of 4–10 indicate the origin of aquatic OM source, whereas C/N ratios of >20 typically indicate dominant contribution of terrestrial plants (Meyers and Ishiwatari, 1993). However, the use of C/N ratios as OM source indicator can be biased since C/N ratios can be altered during degradation. This can shift the C/N ratio to higher values if the degraded OM is enriched in labile nitrogen rich compounds like proteins, peptides, and free amino acids, which are most abundant in planktonic OM. On the other hand, OM of terrestrial origin tends to become relatively depleted in carbon during degradation, since nitrogen deficient components like carbohydrates and lipids are preferentially decomposed (Meyers and Lallier-Vergès, 1999). Nevertheless, these alterations are usually of minor magnitude, hence, the source information of the C/N ratio is mainly preserved.

At the modern Lonar Lake, soils show a tendency towards low C/N ratios (Menzel et al., 2013). This is related to the aforementioned preferential degradation of nitrogen depleted components in combination with the immobilisation of re-mineralised nitrogen, which can be absorbed by clay minerals in the form of NH_4^+ (Sollins et al., 1984; Mengel, 1996). This effect has the strongest influence on sediments that show low TOC contents.

The C/N ratio does not provide much direct information for the climate reconstruction. It is particularly useful for determining the OM source, which is not much climate dependent. During wet conditions, more terrestrial OM might be washed into the lake due to denser vegetation and stronger rainfall, but this could also cause more nutrient inwash into the lake promoting the production of aquatic OM. Thus, the C/N ratio cannot be used as a climate proxy but identifies changes in OM source and supports the interpretation of other palaeoclimate proxies that are affected by changes in OM source.

3.5.4. $\delta^{13}C_{org}$

$\delta^{13}C_{org}$ in lake sediments is influenced by the abundances of land plant OM and aquatic OM in the sediments. The $\delta^{13}C$ of terrestrial OM is mainly driven by the percentage of plants using the C_3 pathway and plants using the C_4 pathway of CO_2 assimilation. C_3 plants show $\delta^{13}C$ values of −23 to −35‰, whereas C_4 plants have $\delta^{13}C$ values of −10 to −16‰ (O'Leary, 1988). C_3 plants are more abundant during wet conditions whereas C_4 plants usually spread during phases of dry climate (Tieszen et al., 1979).

$\delta^{13}C$ of the aquatic OM depend on the $\delta^{13}C$ of dissolved inorganic carbon (DIC) and on the concentration of CO_2(aq.) in the photic zone. Lower pCO_2(aq.) leads to reduced fractionation during CO_2 uptake by phytoplankton, and thus to ^{13}C enrichment in aquatic OM (Lehmann et al., 2004). The factors controlling the isotopic composition of DIC in Lonar Lake are i) the aquatic productivity driven by nutrient supply to the lake, ii) redox conditions of surface sediments and lake water, determining the mechanisms and inorganic products of OM decomposition, iii) the pH of lake water, shifting the equilibrium of the three types of DIC (CO_2(aq.), HCO_3^-, and CO_3^{2-}), iv) the development and stability of lake stratification, affecting the exchange of DIC between the euphotic and aphotic zones, and v) CO_2 degassing caused by lake level decline during climatically dry phases. Generally, factors enriching the DIC in ^{13}C are linked to eutrophication, dryer climate, and lake stratification. In highly productive lakes, ^{13}C deficient OM is transported into the sediments, leaving the DIC in the photic zone enriched in ^{13}C (Hodell and Schelske, 1998). This effect can be expedited by strong lake stratification, hampering the convection of lake water, and thus the transport of ^{13}C depleted CO_2, which is produced during OM degradation mostly in the aphotic zone, into the photic zone. Additionally, eutrophic conditions and lake stratification support the development of anoxia in deep waters. This causes the production of highly ^{13}C depleted methane during OM degradation, which can escape the lake system in gaseous state if it is not re-oxidised. Methanogenesis in anoxic sediments is accompanied by the release of ^{13}C enriched CO_2 at the expense of ^{13}C depleted methane. Thus, if methane is degassed from the lake water and not re-oxidised, anoxia leads to enriched $\delta^{13}C$ values of lake water DIC (Gu et al., 2004). In response to dryer climate, evaporation intensifies and the lake level lowers; this increases the salinity, and thus the alkalinity and pH of lake water. Under highly alkaline conditions, the equilibrium of the three types of DIC shifts towards HCO_3^- and CO_3^{2-}, which are enriched in ^{13}C compared to CO_2(aq.) (Zhang et al., 1995). Under these CO_2(aq.) depleted conditions, the growth of phytoplankton capable of using HCO_3^- as carbon source is promoted producing ^{13}C enriched aquatic OM (Stuiver, 1975). Additionally, exceeding evaporation can cause supersaturation of carbonate in the lake water, and consequently CO_2 degassing, which is accompanied by an increase in $\delta^{13}C$ of DIC (Lei et al., 2012).

Since $\delta^{13}C$ increases under dry conditions in both aquatic OM and terrestrial OM, it is a good climate proxy in our record. The only limitation is the influence of lake water anoxia, which more likely occurs in a deeper lake during wet conditions or as a consequence of eutrophication. The anoxia can cause a change in $\delta^{13}C$ of aquatic OM due to methane degassing or methane oxidation, factors that disappear in a shallow oxic lake.

3.5.5. $\delta^{15}N$

The introduction and cycling of nitrogen in lakes involves several dissolved inorganic nitrogen (DIN) species and transformation processes, associated with more or less strong isotopic fractionation. Thus, $\delta^{15}N$ of OM in lakes can exhibit highly diverse values, linked to several processes. Usually, plankton discriminates against ^{15}N during DIN uptake, with the exception of plankton that is capable of fixing molecular nitrogen (Talbot and Lærdal, 2000). Hence, phases of intense phytoplankton blooms are associated with increased $\delta^{15}N$ values of DIN in the photic zone. Comparable to carbon uptake, low concentrations of DIN lead to reduced isotopic fractionation of plankton, amplifying the increase of $\delta^{15}N$ during phases of high aquatic productivity (Peterson and Fry, 1987). However, the most important processes in determining the $\delta^{15}N$ values of DIN, and thus in $\delta^{15}N$ of aquatic OM are the conversion processes of the different DIN species. The most prominent processes are nitrification, denitrification, and ammonia volatilisation, which are associated with strong fractionation factors. Nitrification occurs under oxic conditions and results in ^{15}N depleted nitrate and ^{15}N enriched ammonium, whereas denitrification, occurring under anoxic conditions, leads to ^{15}N enrichment of nitrate at the expense of ^{15}N depleted molecular nitrogen. The strongest fractionating process most probably affecting the DIN pool of Lonar Lake is ammonia volatilisation. This process becomes important in aquatic environments showing high pH values (>9). Under these conditions, the equilibrium between ammonium and ammonia shifts towards ammonia, which is significantly depleted in ^{15}N compared to ammonium (20–35‰) and can escape the water column in gaseous state (Casciotti et al., 2011). Thus, ammonia volatilisation leads to increasing $\delta^{15}N$ values of the remaining DIN in lake water.

Even though terrestrial OM does not contribute as much to the $\delta^{15}N$ variability in lake sediments as to $\delta^{13}C_{org}$ due to the fact that terrestrial OM has much lower nitrogen contents than aquatic OM, changes in $\delta^{15}N$ during phases of low aquatic productivity and high terrestrial OM contribution to the sediments can indicate shifts in the vascular plant and soil nitrogen isotopic composition. In general, $\delta^{15}N$ of soil and terrestrial plant OM increases with increasing temperature and decreasing precipitation (Amundson et al., 2003).

The use of $\delta^{15}N$ as a proxy for climate reconstruction at Lonar Lake is limited since $\delta^{15}N$ values of aquatic OM depend on the redox conditions of lake water with high values occurring under anoxic conditions but also increasing due to high pH. And whereas anoxic water is more likely accompanying high lake levels during wet conditions, the pH increases during dry conditions when ions become concentrated in the shrinking water body. Additionally, terrestrial OM shows a wide range of $\delta^{15}N$ values due to different nitrogen uptake mechanisms, making it difficult to interpret in terms of climate variability.

3.5.6. Amino acids

The monomeric distribution of the amino acids is commonly used to determine the state of OM degradation in sediments. For the assessment of the OM degradation state, we have calculated the Lonar degradation index (LI), which was first calculated for modern Lonar Lake sediments on the basis of the molar percentages of 19 amino acids (Menzel et al., 2013). The LI compares the amino acid assemblage of the core samples with the data set of Menzel et al. (2013), which includes fresh OM like plankton and vascular plants, moderately degraded sediment trap and surface sediment samples, and highly degraded soil samples from Lonar Lake and its catchment. The calculation of the LI follows the approach of the degradation index (DI) calculation developed by Dauwe and Middelburg (1998) and Dauwe et al. (1999):

$$\mathrm{LI} = \sum_i \left[\frac{\mathrm{var}_i - \mathrm{AVGvar}_i}{\mathrm{STDvar}_i} \right] \times \mathrm{fac.coef}_{\cdot i}$$

where var_i is the original mole percentage of each amino acid in the sample, $AVGvar_i$ and $STDvar_i$ are the arithmetic average and the standard deviation and $fac.coef._i$ is the factor coefficient of the first axis of a principle component analysis (PCA) of the individual amino acids in the data set of Menzel et al. (2013). Negative values indicate less degraded and positive values more degraded state of the OM compared to the average of the reference data set.

The second amino acid derived proxy we used is a ratio of individual amino acids that are relatively enriched during aerobic degradation and amino acids that are relatively enriched during anaerobic degradation, named Ox/Anox:

$$\mathrm{Ox/Anox} = \frac{\mathrm{Asp} + \mathrm{Glu} + \beta\text{-Ala} + \gamma\text{-Aba} + \mathrm{Lys}}{\mathrm{Ser} + \mathrm{Met} + \mathrm{Ile} + \mathrm{Leu} + \mathrm{Tyr} + \mathrm{Phe}}.$$

This ratio has been applied to the modern Lonar Lake sediments (Menzel et al., 2013) to evaluate the redox conditions during OM degradation and is based on a study of Cowie et al. (1995).

The amino acid derived indices seem to be good proxies for climate reconstruction as they can be used to identify phases of aerobic degradation within the sediments. Especially during wet phases that induce a deep anoxic lake, elevated values of theses indices identify relatively short term, dry anomalies. Highest values are most probably related to subaerial degradation, and thus to phases of lake desiccation. In rare cases, the indices could be biased by input of eroded soils, which would cause elevated values. In addition, eutrophication causes low LI and Ox/Anox values due to strong aquatic production and the consequent development of lake water anoxia.

4. Results and discussion

The results of our investigation of the biogeochemical and lithological properties of the Holocene sediments from Lonar Lake are shown in Fig. 2. The percentages of the different grain-size classes of the < 200 μm fraction indicate sediments dominated by clayey silt with few exceptions showing sandy silt (Fig. 3). The sandy silt samples are from 863 to 900 cm depth (10.5–7.8 cal ka BP). Based on the changes in biogeochemical properties, lithology, and sedimentation rate, S. Prasad et al. (2014) have identified the large scale climate development over the whole Holocene as well as two phases of prolonged drought. Here we present several shorter phases of climate changes superimposed on the large scale trend. The identified phases of drier and wetter climate can be correlated with other Asian palaeomonsoon records and palaeoclimate records from the North Atlantic region. A detailed description is given below (Section 4.2) after a summary of the large scale climate development with additional remarks regarding the grain-size and amino acid data.

4.1. Large scale Holocene climate transition

The general long term palaeoclimate trend at the climatically sensitive Lonar Lake reconstructed by S. Prasad et al. (2014) starts with a drying period that probably coincides with the Younger Dryas at ~11.4 cal ka BP, which marks a dry period prior to the beginning of the Holocene in many geological records of India and adjacent regions (Overpeck et al., 1996; Bar-Matthews et al., 1997; Wei and Gasse, 1999; Gasse, 2000; Wang et al., 2001; Morrill et al., 2003; Sharma et al., 2004; Dykoski et al., 2005; Demske et al., 2009). Median grain-

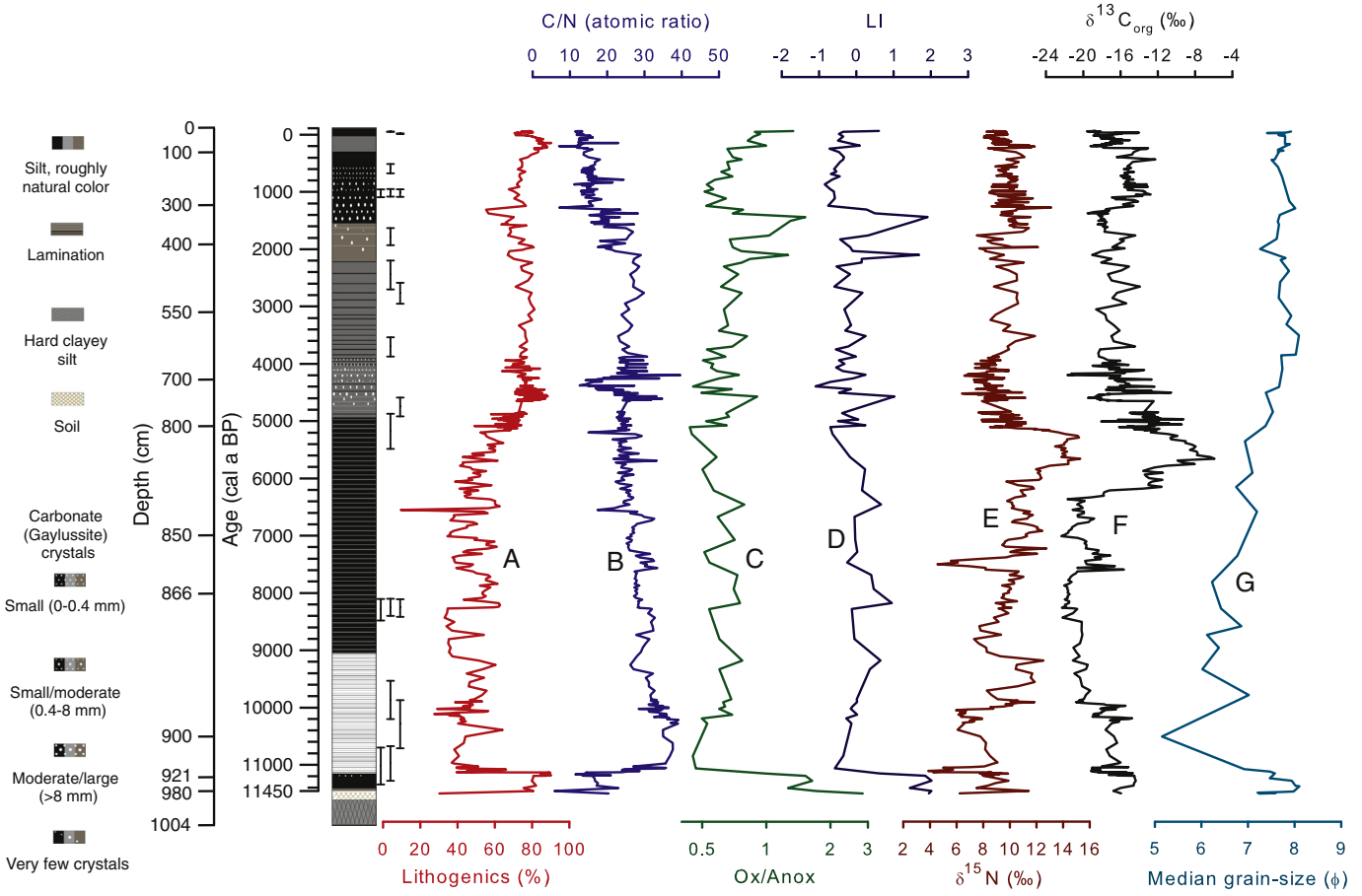

Fig. 2. Summary of the analytical results. Schematic lithology of the Lonar Lake core and down-core variation in lithogenic contribution (A), C/N ratio (B), amino acid derived indices Ox/Anox (C) and LI (D), stable nitrogen (E) and carbon (F) isotopic ratios of bulk organic matter, and median grain-size of the < 200 μm fraction (G). C/N, $\delta^{13}C_{org}$, and $\delta^{15}N$ were reported by S. Prasad et al. (2014); gaylussite crystal occurrence was reported by Anoop et al. (2013b). Error bars indicate the standard deviation range (2σ) of calibrated radiocarbon dates.

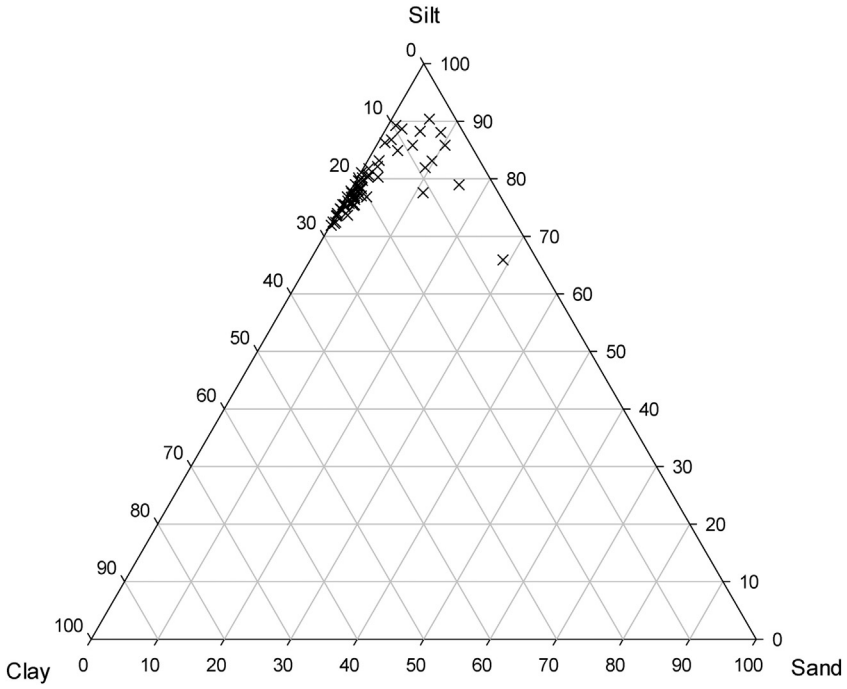

Fig. 3. Ternary diagram showing the percentages of the different grain-size classes (clay, silt, sand) of the < 200 μm fraction of the analysed Lonar Lake core sediment samples.

size of this section is small indicating low energy transport, which is probably due to dry conditions with reduced sediment input by run-off and precipitation fed streams and enhanced aeolian deposition. High LI values indicate strongly degraded OM in these sediments, and the high Ox/Anox ratios point to subaerial decomposition of the OM. Thus, the bottommost sediment section most likely represents a palaeosol.

The beginning of the Holocene is marked by a transition from dry to wet climate with an abrupt increase in monsoon strength after ~11.4 cal ka BP (S. Prasad et al., 2014). The phase of monsoon onset

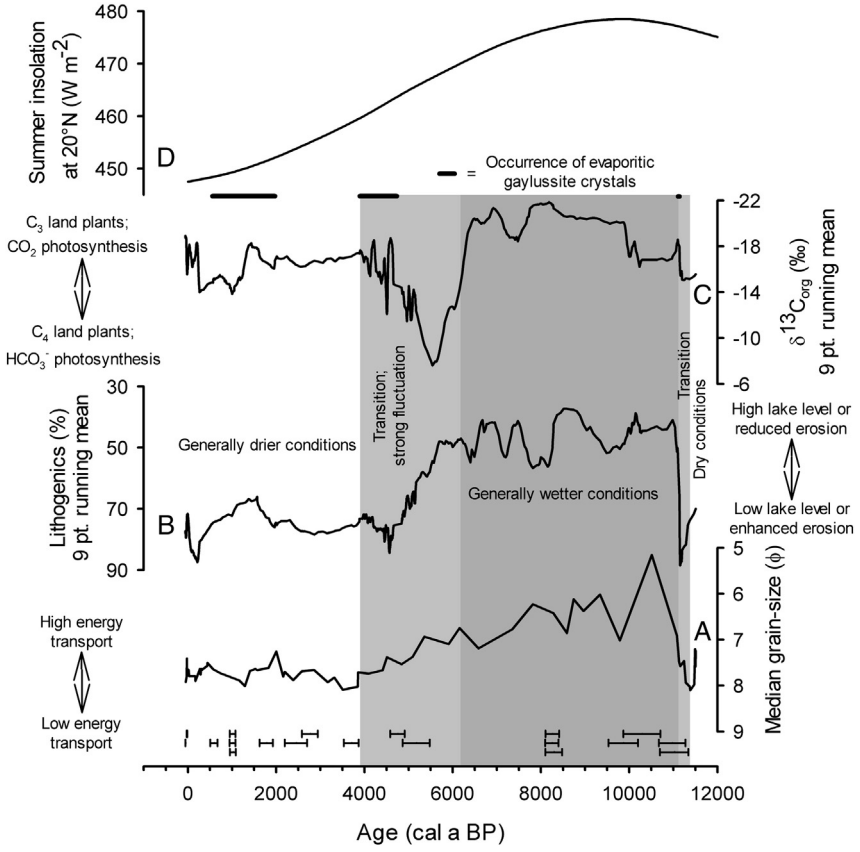

Fig. 4. Long term Holocene climate trend at Lonar Lake as interpreted from our data. Comparison of median grain-size of the < 200 μm fraction (A), lithogenic contribution (B), $\delta^{13}C_{org}$ values (C) (S. Prasad et al., 2014), and summer (JJA) insolation at 20° N (D) (Berger and Loutre, 1991). Error bars indicate the standard deviation range (2σ) of calibrated radiocarbon dates.

and strengthening is reflected in the sediments by high lithogenic input, which was eroded from the sparsely vegetated crater walls and transported to the dried out lake bed. The values of the biogeochemical parameters and the grain-sizes are comparable to those of the underlying soil, and thus indicate high contribution of eroded soil material to the sediments. On top of this section, few gaylussite crystals can be found, denoting a drier phase at ~11.1 cal ka BP.

Subsequently, the early Holocene between 11.1 and 6.2 cal ka BP is characterised by wet conditions (Fig. 4). The sediments of this section show relatively low lithogenic contribution, and consequently low sedimentation rates. Thus, the section represents a deep lake with less eroded material reaching the sampling site. A deep lake developed quickly after 11.1 cal ka BP as is obvious from seasonally laminated sediments (S. Prasad et al., 2014). The median grain-size values indicate a shift to medium silt, and thus to slightly coarser material. This might be due to higher energy transport during strong rainfall events. The aquatic productivity was low during this phase, as shown by the high C/N ratios (mean = 30.1), which denote dominant contribution of terrestrial OM. Since 9.9 cal ka BP the $\delta^{13}C_{org}$ values stabilised on a relatively low level (mean = −20.9‰) indicating a C_3 dominated vegetation in the catchment of the lake. The predominantly low LI and Ox/Anox values of the section and the increasing $\delta^{15}N$ values between 9.1 and 6.2 cal ka BP point to extended anoxia in the water column and the sediments.

The time slice between 6.2 and 3.9 cal ka BP is regarded as being a transitional phase between wet climate during the early Holocene and dry climate during the late Holocene. This time slice shows two drying phases accompanied by strong water body reduction between 6.2 and 5.2 cal ka BP and between 4.6 and 3.9 cal ka BP, respectively. The former drying phase is most obvious from high $\delta^{13}C_{org}$ and $\delta^{15}N$ values, whereas the latter shows elevated lithogenic contribution and gaylussite crystal precipitation (Fig. 4), which indicates strongest lake level decline.

Following the climate transition between 6.2 and 3.9 cal ka BP, evidence of relatively dry climate persists until today. Elevated $\delta^{13}C_{org}$ values, lithogenic contribution, Ox/Anox ratios, and finer median grain-sizes indicate drier conditions compared to the early Holocene. The lithogenic contribution and the Ox/Anox ratios denote a shallow lake, and the $\delta^{13}C_{org}$ values imply a dominance of C_4 catchment vegetation. The grain-size data indicate weaker monsoon rains causing lower transport energy. Additionally, the alluvial fan in the northeast of the lake might have been exposed due to the lower lake level, possibly reducing the velocity of the streams that enter the lake from the northeast and east. Probably, this effect has also reduced the distance between the sampling site and the source of fine sediment (alluvial fan/stream mouth) causing a shift to finer grain-sizes and increasing the sedimentation rate. A phase ofexceedingly dry conditions is indicated by the reoccurrence of evaporitic gaylussite crystals between 2.0 and 0.6 cal ka BP (Anoop et al., 2013b; S. Prasad et al., 2014). The climate information of the younger part of the core might be mirrored to some extent due to anthropogenic interferences, as for example eutrophication and deforestation. A persistent decrease in C/N ratio since 1.3 cal ka BP indicates permanently elevated nutrient supply to the lake, which cannot be observed in the older parts of the core. Thus, a natural source of these additional nutrients seems unlikely. Since ca. 0.8 cal ka BP strong anthropogenic interference is evident from several near shore temples that have been built during the Yadavan rule approximately in the 12th century (Malu et al., 2005).

In general, the impact of long term Holocene climate change on palaeolimnology becomes notably obvious from the $\delta^{13}C_{org}$, lithogenic contribution, and grain-size values in our record and quite well delineates the insolation curve since the end of the Younger Dryas (Fig. 4), which additionally seems to drive the position of the summer Inter-Tropical Convergence Zone (ITCZ), and thus the strength and northwards extent of the summer monsoon rainfall (Fleitmann et al., 2007). One point that might be questioned is the characteristic of the climate deterioration at 6.2 cal ka BP, which is reflected in the Lonar Lake record by a sharp increase in $\delta^{13}C_{org}$, and thus points to an abrupt change, which was also reported from other records (Morrill et al., 2003). Nevertheless, we believe that this abrupt change is related to short term climate variability and that the sudden increase in $\delta^{13}C_{org}$ at 6.2 cal ka BP most likely represents the transgression of a threshold in annual precipitation that led to the decline in terrestrial C_3 plant vegetation and the increase in C_4 plant contribution. Also, the changes in lake level as displayed by the lithogenic content in the sediments show a relatively smooth transition from a deep to a shallow lake. Additionally, the relatively short term of the interval of drying between 6.2 and 3.9 cal ka BP is obvious from the subsequent change to wetter conditions indicated by subaquatic sedimentation and the disappearance of the gaylussite minerals. Thus, the transition from generally wet to drier climate after the Holocene climate optimum seems to occur gradually, and abrupt changes in the biogeochemical parameters are due to relatively short-term climate anomalies as postulated by Fleitmann et al. (2007) and reported from several regions (Hodell et al., 1999; Gupta et al., 2003; Hong et al., 2003; Gupta et al., 2005; Demske et al., 2009; Wünnemann et al., 2010).

4.2. Centennial scale Holocene climate variability

Besides the large scale millennial climate trend, several smaller centennial scale climate variations can be reconstructed from the Lonar Lake bioclastic record. While the role of ENSO and shifts in the position of the Indo Pacific Warm Pool (IPWP) in causing the prolonged droughts during 4.6–3.9 and 2.0–0.6 cal ka have been discussed by S. Prasad et al. (2014), the short term climate variability identified in our new dataset cannot be explained by the same mechanism necessitating the search for alternative causal mechanisms. Several studies have identified links between Asian monsoon and North Atlantic palaeoclimate with cold events in the North Atlantic region, as identified by ice-rafted debris in deep sea cores (Bond et al., 1997; Bond et al., 2001), being linked to decreases in monsoon strength over Asia (Gupta et al., 2003; Hong et al., 2003; Dykoski et al., 2005; Wang et al., 2005; Fleitmann et al., 2007). Nearly all Bond events are isochronally reflected by indications of short term changes in monsoon strength in the proxies from Lonar Lake sediment core (Fig. 5). Since the centennial scale climate variations at Lonar Lake are reflected in different proxies and not all proxies show every phase of climate change, we calculated a Bioclastic Climate Index (BCI) that combines the Holocene course of the independent and climatically sensitive $\delta^{13}C_{org}$, lithogenic contribution, and combined amino acid proxy values. Since the variations in $\delta^{15}N$ and C/N values within the Lonar Lake record seem not to be predominantly driven by climate change or at least are considerably biased by other processes (see Sections 3.5.3 and 3.5.5), we did not include them into the BCI calculation. The BCI shows the deviation from the mean values given in percent of the maximum variation of the respective proxy in the data set according to the formula:

$$\mathrm{BCI}\ (\%) = \frac{\Delta^{13}\mathrm{C}\ (\%) + \Delta\mathrm{lith}\ (\%) + 0.5 \times [\Delta\mathrm{LI}\ (\%) + \Delta\mathrm{Ox/Anox}\ (\%)]}{3}$$

with high values indicating drier and low values indicating wetter conditions. We used half of the sum of the LI and Ox/Anox values to not overstate the variability in amino acid data as both values are calculated from the same data set, and thus are not fully independent. Further, linearly interpolated values for the amino acid derived proxies were used as these proxies were measured in a lower resolution than $\delta^{13}C_{org}$ and lithogenic contribution. Since the BCI also shows the long term palaeoclimate trend, a detrended curve was calculated to emphasise the centennial scale palaeoclimate variations (Fig. 6). The applicability of the BCI in reconstructing changes in precipitation is corroborated by its negative correlation (−0.55; $p < 0.01$), despite human interferences at Lonar Lake in modern times, with the all India rainfall record (ftp://www.tropmet.res.in/pub/data/rain/iitm-regionrf.txt) by applying a low-pass filter to the rainfall data and the Gaussian kernel based correlation analysis (NESToolbox for MATLAB used; Rehfeld et al., 2011). In addition to the BCI, the occurrence of evaporitic gaylussite crystals (Anoop et al., 2013b)

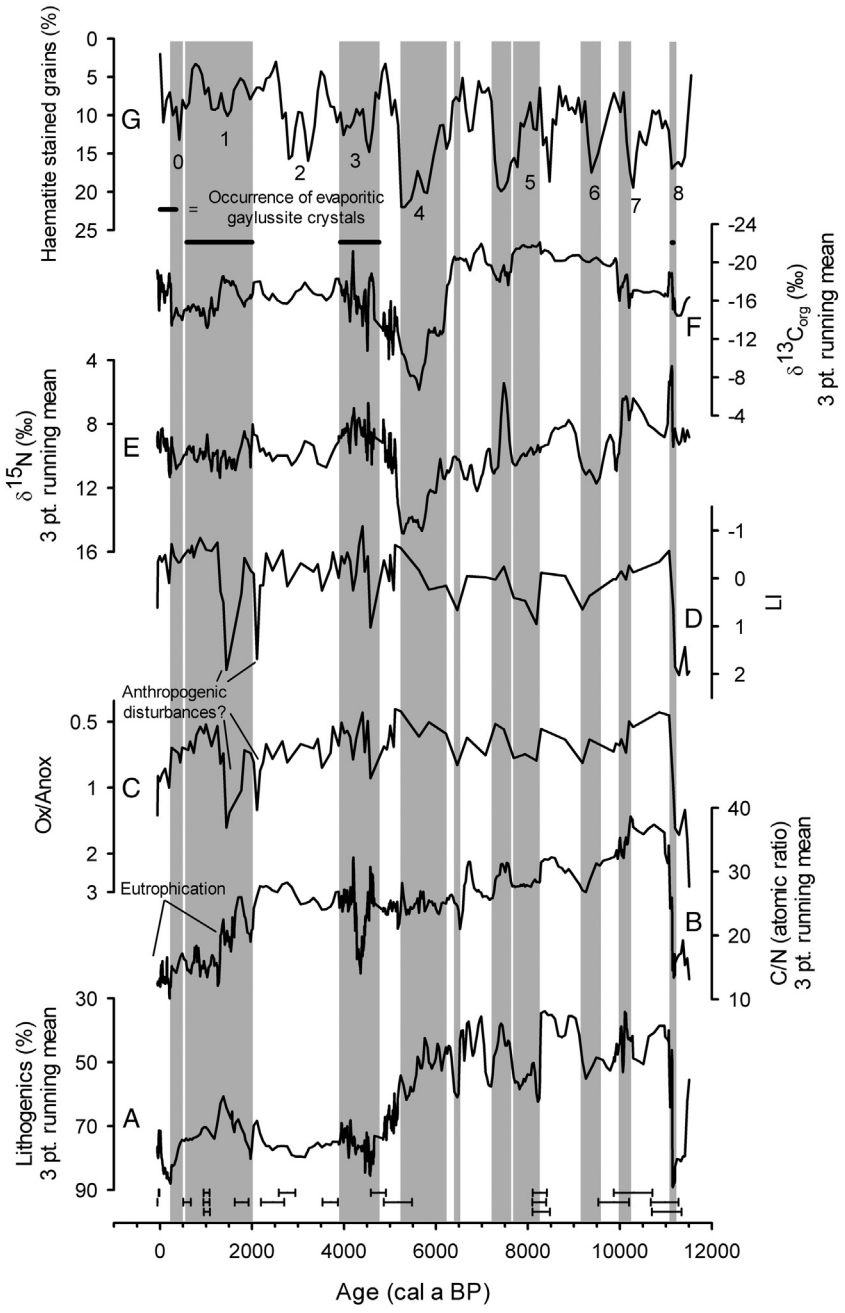

Fig. 5. Comparison of our data of lithogenic contribution (A), C/N ratio (B), Ox/Anox ratio (C), LI (D), $\delta^{15}N$ (E), and $\delta^{13}C_{org}$ (F) to the percentage of haematite stained grains (G) in core MC52, a climate record from the North Atlantic region (Bond et al., 2001). C/N, $\delta^{13}C_{org}$, and $\delta^{15}N$ were reported by S. Prasad et al. (2014); gaylussite crystal occurrence was reported by Anoop et al. (2013b). Numbers 0–8 designate cold events in the North Atlantic region (Bond events). Grey shaded intervals denote periods that are interpreted to be phases of climate deterioration at Lonar Lake. Error bars indicate the standard deviation range (2σ) of calibrated radiocarbon dates.

was used to interpret the climatic changes at Lonar Lake since the gaylussite crystals exclusively indicate changes in Lonar Lake hydrology related to reduced available effective moisture.

Largely, the changes in the de-trended BCI are coincident with the intervals of increased ice rafted debris in the North Atlantic (Bond et al., 2001). The oldest of the Holocene cooling events in the North Atlantic region, the Bond event 8, can be correlated with the occurrence of gaylussite crystals in the Lonar Lake core on top of the section that represents the phase of climate transition and monsoon onset after the soil formation (Fig. 5). The Bond event 7 is concurrently correlated to a double-peaked increase in $\delta^{13}C_{org}$ and to an increase in lithogenic contribution. The $\delta^{13}C_{org}$ increases are interpreted as changes in terrestrial vegetation to more C_4 plant abundance, indicating drier conditions. The subsequent decrease in $\delta^{13}C_{org}$ denotes the transition to C_3 plant domination, and thus wetter conditions during the early Holocene. A concurrent climate variation to Bond event 6 is indicated by elevated LI and Ox/Anox values as well as high $\delta^{15}N$ values (Fig. 5). The amino acid based indices reveal an increase in oxygen supply to the sediments at 9.15 cal ka BP, and the pollen record points to a dry phase, during which the whole sediment section of this subunit became exposed to oxic or even subaerial conditions, since only few pollen that are resistant to aerobic decomposition are preserved in the sediments older than 9.2 cal ka BP (Riedel & Stebich, unpublished data). Enhanced oxygen supply could also be responsible for the elevated $\delta^{15}N$ values, since an

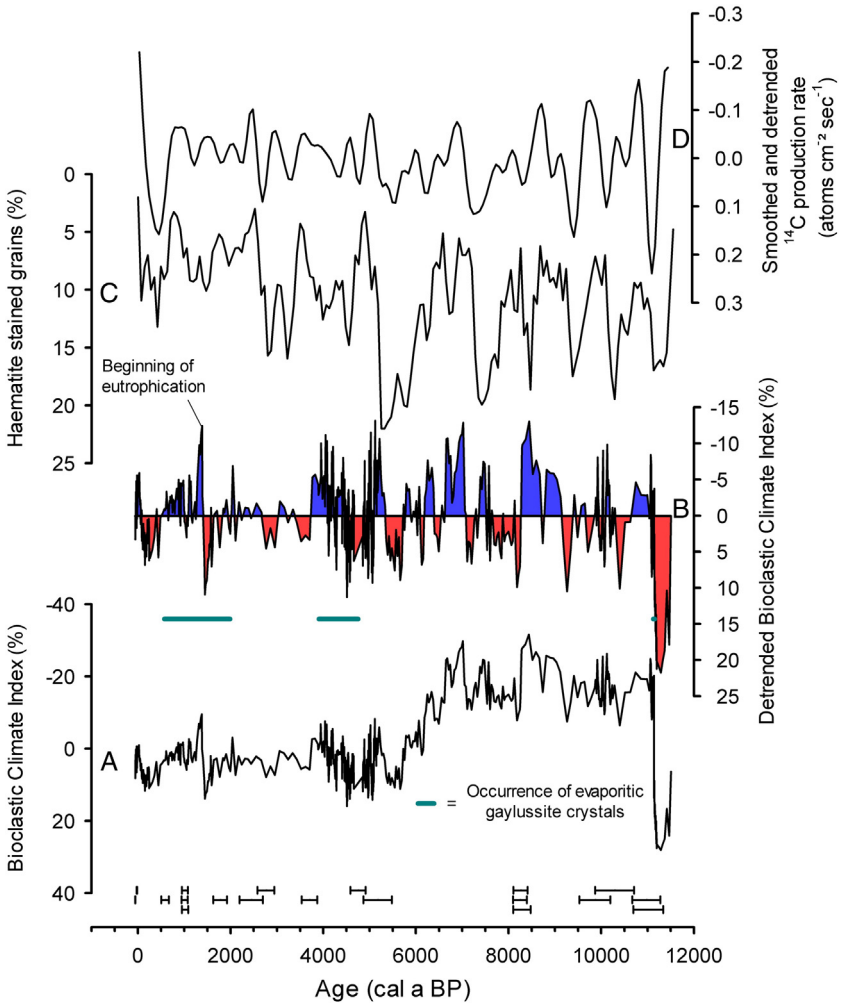

Fig. 6. Comparison between the Bioclastic Climate Index (BCI) (A), the detrended BCI (B), the climate record from the North Atlantic Region (C), and the detrended and smoothed ^{14}C production rate (D) (Bond et al., 2001). Detrending of the BCI was performed by applying a Gaussian kernel based filter with a kernel bandwidth of 500 years to the values of the time slice <11.14 cal ka BP. The values of the time slice ≥11.14 cal ka BP were adjusted by subtracting the lowest value of this time slice from the data since a rapid shift in BCI values at 11.14 cal ka BP occurs. Red and blue colour fills indicate relatively dry and wet phases, respectively. Error bars indicate the standard deviation range (2σ) of calibrated radiocarbon dates. (For interpretation of the references to colour in this figure legend, the reader is referred to the web version of this article.).

increase in $\delta^{15}N$ during aerobic degradation was reported from in vitro (Lehmann et al., 2002) as well as from in vivo (Freudenthal et al., 2001) investigations. A drying trend in the Asian tropical region during this so called 9.2 ka event was reported before and also related to a cooling trend in the North Atlantic region (Dykoski et al., 2005; Fleitmann et al., 2008). Elevated LI, Ox/Anox, and lithogenic contribution values in the Lonar Lake core comparable to the values at 9.2 cal ka BP can be found during 8.2–7.7 cal ka BP (Fig. 5). This phase correlates within dating uncertainties with a cool phase in the North Atlantic situated at the early stage of Bond event 5. The relatively short cool phase during the early stage of Bond event 5 is also known as the 8.2 ka event. Similar to the 9.2 ka event, a cooling trend in the North Atlantic region was accompanied by a drying trend in monsoon-influenced Asia (Alley et al., 1997; Wang et al., 2005). It is widely accepted that the cooling during the 8.2 ka event was caused by a pulse of freshwater that burst out of the Lakes Agassiz and Ojibway through the Hudson Straight, which weakened the thermohaline Atlantic meridional overturning circulation, thus leading to the climate anomaly (Barber et al., 1999; Teller et al., 2002; Kendall et al., 2008). The peak at the later stage of Bond event 5 is correlated with elevated $\delta^{13}C_{org}$ values and an increase in lithogenic contribution (Fig. 5). Elevated LI, Ox/Anox, and lithogenic contribution at 6.45 cal ka BP correlate within dating uncertainties with a cool phase at the beginning of Bond event 4. The following intensification of the North Atlantic cold spell (Bond event 4) and the Bond event 3 are reflected by the most obvious centennial scale climate changes shown by our data. These two phases constitute the climate transition from generally wet to generally drier conditions during the mid Holocene (see Section 4.1) at 6.2–5.2 cal ka BP and 4.6–3.9 cal ka BP, respectively, which is consistent with reports of southward migration of the ITCZ, monsoon weakening, and related drying trends from various locations of the Asian monsoon realm (Enzel et al., 1999; Morrill et al., 2003; Parker et al., 2004; Prasad and Enzel, 2006; Staubwasser and Weiss, 2006; Fleitmann et al., 2007; Demske et al., 2009; V. Prasad et al., 2014). The older phase, concordant with Bond event 4, is characterised by a strong increase in $\delta^{13}C_{org}$ with two sudden shifts, the first by ~8‰ at about 6.2 cal ka BP and the second by ~4‰ at about 5.7 cal ka BP. The second shift in $\delta^{13}C_{org}$ is accompanied by an increase in $\delta^{15}N$ of ~2‰. The increase in $\delta^{13}C_{org}$ is most likely linked to two major factors. A shift in terrestrial vegetation from C_3 dominance to more C_4 contribution seems to explain the increase in $\delta^{13}C_{org}$ at 6.2 cal ka BP since S. Sarkar (in preparation) found an increase in $\delta^{13}C$ of long chain n-alkanes. The second increase in $\delta^{13}C_{org}$ at 5.8 cal ka BP results in $\delta^{13}C_{org}$ values that even exceed the values of C_4 land plants, and thus the second shift cannot be explained by a further change in the terrestrial fraction of the OM alone. Hence, the elevated $\delta^{13}C_{org}$ values seem to be related to a change in the aquatic system. A reasonable explanation is an increase in pH, as a result of an increased salt concentration in the water during lake level decline in response to

relatively dry conditions, and a related shift in the dominant photosynthetic inorganic carbon source from CO_2 to HCO_3^- (S. Prasad et al., 2014). The assumption that elevated pH is responsible for the $\delta^{13}C_{org}$ increase is corroborated by the concurrent increase in $\delta^{15}N$. In anoxic waters, which most probably were present during the related time as indicated by the low Ox/Anox ratios, high pH causes ammonia volatilisation that leads to a $\delta^{15}N$ increase of aquatic OM (Casciotti et al., 2011). After 5.2 cal ka BP, the $\delta^{13}C_{org}$ and $\delta^{15}N$ values gradually decrease, which could indicate a slightly wetter period from 5.2 to 4.6 cal ka BP but which could also be due to the disappearance of the anoxic water layer as a response to further lake level decline. Subsequently, the dry phase between 4.6 and 3.9 cal ka BP, which has been correlated with an expansion of the IPWP (S. Prasad et al., 2014) but also partly correlates with Bond event 3, does not show as elevated $\delta^{13}C_{org}$ and $\delta^{15}N$ values as the previous dry episode. This seems to be related to the disappearance of the anoxic water layer, and hence the lack of ammonia volatilisation, producing ^{15}N enriched ammonium, and the lack of methanogenesis, producing ^{13}C enriched CO_2. The strongest indications for dry climate during this period are the occurrence of evaporitic gaylussite crystals throughout this zone (Anoop et al., 2013b) and the elevated lithogenic content in the sediments indicating low lake level. However, the decreased $\delta^{13}C_{org}$ values are responsible for the lower BCI values during this time slice even though the occurrence of gaylussite crystals indicates drier conditions compared to the time slice 6.2–5.2 cal ka BP (Fig. 6). Subsequently, the only Bond event that does not show a marked complement in the Lonar Lake record is Bond event 2 between ca. 3.5 and 2.7 cal ka BP. This might be due to the fact that generally drier conditions had been established after the very dry period correlated with Bond events 4 and 3. Thus, the wetter period during ca. 3.9–3.5 cal ka BP did not provide enough excess in precipitation over evaporation to establish a high lake level with strong anoxic hypolimnion and vegetation dominated by C_3 plants. Hence, if the period between 3.5 and 2.7 cal ka BP was drier at Lonar Lake compared to the period 3.9–3.5 cal ka BP, no significant changes in our proxies could be expected as long as the lake does not desiccate. Nevertheless, two minor positive shifts in $\delta^{13}C_{org}$ and contemporaneous increases in the amino acid derived indices result in two BCI peaks that possibly indicate drier conditions at Lonar Lake corresponding to the double-peaked North Atlantic cooling event during Bond event 2 (Fig. 6). The following period of strong evidence of climate deterioration at Lonar Lake is again marked by evaporitic gaylussite crystals and was dated at an age of 2.0–0.6 cal a BP (Anoop et al., 2013b; S. Prasad et al., 2014). Thus, it can be correlated with Bond event 1 but exceeds the time span of the Bond event by about 500 years, which is in accordance with the report of decadal scale famines in India during the 14th and 15th century (Sinha et al., 2007). However, this strong drying event is also coincident with an increase in ENSO like conditions (Moy et al., 2002; Rein et al., 2005) in the Pacific (S. Prasad et al., 2014) suggesting complex links to the North Atlantic and to the Pacific forcings. The dry climate of this period, as indicated by the gaylussite precipitation, is not well reflected in the BCI. This is due to the eutrophication, which causes the development of lake water anoxia and a related descent of the amino acid derived proxy values. The BCI indicates an abrupt transition to wet climate at 1.3 cal ka BP (Fig. 6), which is due to the biased amino acid indices. Thus, the BCI values during the phase of strongest anoxia between 1.3 and 0.3 cal ka BP, as indicated by the Ox/Anox ratio, are shifted to lower values, hence indicating wetter climate than actually prevailed. Finally, Bond event 0 is concurrently correlated to increased $\delta^{13}C_{org}$ and lithogenic contribution values between 440 and 240 cal a BP (Fig. 5). Again, anthropogenic interference cannot be ruled out here in the younger part of the core. But, since the two-step increase in $\delta^{13}C_{org}$ at 440 and 260–245 cal a BP and the subsequent decrease in $\delta^{13}C_{org}$ correlate with two minima in solar activity, the Spörer Minimum and the Maunder Minimum, and a subsequent increase in solar activity, it seems likely that these changes are driven by monsoon strength weakening during the 'Little Ice Age' (Bond event 0) and the subsequent climate amelioration (Anderson et al., 2002; Agnihotri et al., 2008).

Multiple proxies (S. Prasad et al., 2014; this study) indicate that there are both tropical and high latitude influences on the ISM that can be finally linked to solar variability. The fact that all phases of climate cooling in the North Atlantic region identified by Bond et al. (2001) are largely contemporaneously (within dating uncertainties) accompanied by climate deteriorations at Lonar Lake, as inferred from changes in BCI and evaporative gaylussite crystal precipitation, indicates that the North Atlantic and the Indian monsoon climate systems were linked during the Holocene. Evidence for contemporaneous climate variability in the Asian tropics and the North Atlantic region during the Holocene has also been reported from annually laminated, precisely dated stalagmites (Liu et al., 2013). A reasonable explanation for such a concurrent linkage is an atmospheric tele-connection, which has the potential to connect the two systems without substantial delay. Coupled ocean–atmosphere climate simulations could show that cooling of the northern hemisphere results in reduced summer monsoon rainfall over India (Broccoli et al., 2006; Pausata et al., 2011). This is due to the development of an asymmetric Hadley cell accompanied by a southwards shift of the ITCZ, which causes an enhanced net energy (heat) transport from the tropics to the cooled northern hemisphere (Broccoli et al., 2006). Such a southwards shift of the ITCZ would lead to weaker-than-normal Asian summer monsoon, and thus might be the mechanism responsible for the Asian-North Atlantic climate connection indicated by our data. Another mechanism that might have contributed to the connection could be the effect of northern hemisphere cooling on Eurasian snow cover if the cold phases recorded in the North Atlantic region have caused enhanced snow accumulation over Eurasia. Modern observations and model calculations show that extent and duration of Eurasian snow cover affect the Asian monsoon system (Barnett et al., 1989; Bamzai and Shukla, 1999). Prolonged Eurasian snow cover during spring cools the overlying air since energy is used to melt the snow and to evaporate the melt water instead of warming the land surface, thus having a downwind effect on South Asian landmasses and weakening the thermal gradients between land and ocean, which causes a weaker-than-normal summer monsoon (Barnett et al., 1989).

The reason for the North Atlantic cooling events might be reduction in insolation triggered by reduced solar output. This was postulated by Bond et al. (2001) who found that the North Atlantic cooling events correlate with smoothed and detrended ^{14}C and ^{10}Be production rates (^{14}C shown in Fig. 6), which are inversely correlated with solar output (Beer, 2000). They also found a ca. 1500 year periodicity of the palaeoclimate variation in their record, which is in agreement with palaeoclimate variations reconstructed from other records (see Mayewski et al., 2004) and the link between periodicities in climate archives and solar activity (Soon et al., 2014). To compare these findings with our data, we have calculated the major frequencies in our climate proxy data as well as the correlation between the BCI and the ^{14}C production rate. Before the spectral analysis, the long term climate trend was removed from the whole time series by applying a Gaussian kernel based filter with a kernel bandwidth of 500 years. The correlation between the detrended ^{14}C production rate (Bond et al., 2001) and the detrended BCI is relatively high (0.63), thus supporting the hypothesis that climate variability in India is influenced by changes in solar irradiance (Gupta et al., 2005). The power spectral analysis revealed a 1519 year periodicity besides 120 year, 274 year, 435 year, and 822 year periodicities in our data set (Fig. 7). Thus, a periodicity in climate variability similar to the "1500-year cycle" observed by Bond et al. (2001) is present in our record and corroborates the connection of the North Atlantic and the Indian monsoon palaeoclimates. The other periodicities seem to be related to solar cycles. The periodicities of 120 and 435 years equal eccentricity periodicities (122 and 432 years), whereas the 822 year cycle might be related to precession and obliquity cycles of 840 years (Loutre et al., 1992). Due to the difference, it is questionable if the

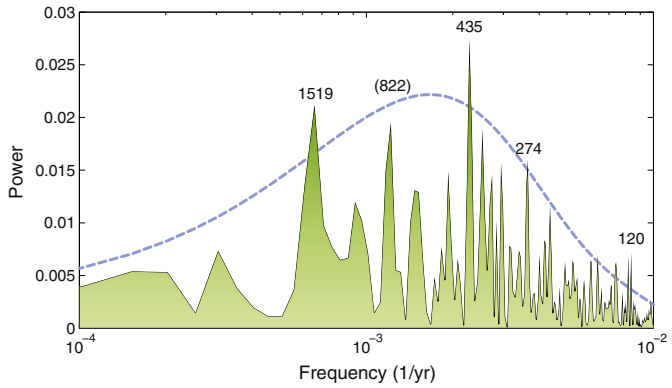

Fig. 7. Powerspectrum indicating the most prominent periodicities within the Bioclastic Climate Index data set. The blue line represents the 90% confidence level of statistical significance. (For interpretation of the references to colour in this figure legend, the reader is referred to the web version of this article.).

274 year cycle in our data set is related to the 245 year cycle of eccentricity, obliquity, and precession (Loutre et al., 1992), but the possibility should not be excluded. In summary, we conclude that while IPWP forcings are important in causing millennial scale periods of prolonged dryness during the mid and late Holocene in central India (S. Prasad et al., 2014), the subtle short term changes identified by the BCI indicate the presence of North Atlantic forcings as well.

4.3. Implication for the archaeological history

Our palaeoclimate reconstruction from Lonar Lake gives some clues according to the ongoing discussion about the role of mid-Holocene climate change on the de-urbanisation and abandonment of most Mature Harappan cities in the Indus valley region and the dislocation of settlements during the Late Harappan phase after 3.9 cal ka BP especially to the western Ganga Plains (Possehl, 1997). Singh (1971) postulated that the development and expansion of the Harappan Civilisation was strongly related to favourable climate conditions and to severe climate deterioration during its decline. However, Possehl (1997) and Enzel et al. (1999) proposed that the influence of climate to the fate of the Harappan Civilisation was minimal or absent. But, since the capture of rivers that contributed to the water supply of the Harappan cities caused by tectonic activity during the time of Harappan decline could not be confirmed (Clift et al., 2012) and since almost all of these rivers were monsoon fed (Tripathi et al., 2004; Giosan et al., 2012), vulnerability of the urban Harappan sites to weakened monsoon seems likely. And while Staubwasser and Weiss (2006) argue for a direct link between the decline of the Harappan Civilisation and the relatively short dry episode at about 4.2 cal ka BP, others hypothesise that the gradual climatic decline between ~5 and 4 cal ka BP caused an adaption of the cultivation methods to reduced summer monsoon rainfall (Gupta et al., 2006; Madella and Fuller, 2006; MacDonald, 2011) and related diminution in seasonal flooding (Giosan et al., 2012).

Our data support the view that the rise of the Harappan Civilisation did not occur during a phase of wettest climate (Enzel et al., 1999) but that the development of the huge cultural centres was more likely linked to the climate deterioration during the transition from the wetter early Holocene towards the drier late Holocene. A similar development was reconstructed for the rise and fall of the Mayan cities in Central America where the spread of urban centres coincided with a phase of declining humidity between 1.3 and 1.15 ka BP and the abandonment started subsequently at ~1.15 ka BP probably due to persistent dry conditions (Kennett et al., 2012). The development of highly populated centres in the Indus Valley was possibly due to the reduction of annual rainfall and the concentration of cultivable acreage along the rivers that provided enough water for agriculture in the form of seasonal flooding to supply the resident population. The fact that diminished available effective moisture at Lonar Lake between 4.6 and 3.9 cal ka BP correlates well with other records from the Asian monsoon realm (Hong et al., 2003; Gupta et al., 2005; Demske et al., 2009; Wünnemann et al., 2010) displays the supra-regional character of this drying trend and corroborates the assumption that the climatically sensitive sites especially in the relatively dry regions of the western Harappan territories were forced to adapt to severe shortages in water supply as for example to rivers that became ephemeral. A consequent change in agricultural strategy towards cultivation of crops that called for a more extensive land use and could not support the highly populated centres seems to be a reasonable explanation for the gradual decline of the Harappan Civilisation.

5. Conclusions

The analyses of the C/N, $\delta^{13}C_{org}$, $\delta^{15}N$, lithogenic contribution, grain-size, and amino acid degradation indices LI and Ox/Anox ratio values in combination with the evaporitic gaylussite crystals from the sediment core samples of the climatically sensitive Lonar Lake revealed several environmental and hydrological changes during the Holocene that can be related to climate shifts.

The long term Holocene climate development at Lonar Lake shows three phases. The first phase is characterised by dry conditions at about 11.4 cal ka BP followed by a transition to wetter conditions during the time of monsoon onset and strengthening (~11.4–11.1 cal ka BP). The second phase comprises the early Holocene and shows wet conditions with high lake level and C_3 dominated catchment vegetation. A subsequent transition to drier conditions occurs between ca. 6.2 and 3.9 cal ka BP. The late Holocene represents the third phase, which is characterised by relatively dry conditions as indicated by lower lake level and terrestrial vegetation with high C_4 plant contribution. Comparison of these findings with other climate records from South Asia and the North Atlantic region displays a strong similarity, with strong monsoon phases in Asia correlating with warm periods in the North Atlantic region and weak monsoon correlating with colder climate in the North Atlantic region (Johnsen et al., 2001). These climatic conditions seem to be closely related to the northern hemisphere insolation, which additionally seems to drive the position of the ITCZ, and thus the northwards extent of the summer monsoon rainfall (Fleitmann et al., 2007).

The long term climate trend is superimposed by several shorter term climate fluctuations. Some of these fluctuations have also been observed in other high resolution climate records from Asia, and they can be correlated with the North Atlantic Bond events (Bond et al., 1997, 2001). The correlation is the same as observed for the long term trend with cold periods in the North Atlantic correlating with dry periods over South Asia and vice versa. All the 9 Bond events during the Holocene are isochronally (within dating uncertainties) reflected in the Lonar Lake record. This points to a connection between the two climate systems or to an identical trigger of climate variability. The fact that the Bioclastic Climate Index (BCI) quite well delineates the solar output proxy ^{14}C production rate (Bond et al., 2001) corroborates the assumption that variations in solar activity triggered centennial scale variability of the Indian monsoon climate during the Holocene. However, the amplitude of the BCI not solely depends on the centennial climate variability but is also influenced by the long term Holocene climate variability, other tele-connections (e.g., Pacific climate; S. Prasad et al., 2014), local climate phenomena, changes in environmental conditions, and anthropogenic interferences. Thus, the amplitude of the BCI curve does not always reliably display the absolute strength of climate variability.

With respect to the archaeological record from India and Pakistan, our results support the hypothesis that the rise of the Harappan Civilisation was linked to the climate deterioration during the transition from wetter climate of the early Holocene to drier climate of the late Holocene. We believe that the decline of the urban centres especially in the western Harappan territories might best be explained by a gradual reduction of summer monsoon between ~4.6 and 3.9 cal ka BP and a

consequent adoption of new agricultural practices and crops that demanded a social adjustment.

Acknowledgements

The authors like to thank R. Niederreiter of UWITEC in Mondsee, Austria and K. Deenadayalan and Md. Arif of the IIG in Mumbai for their support during field work, F. Langenberg and N. Lahajnar of the IfGeo in Hamburg and U. Kegel of the GFZ for their assistance during laboratory analyses. Special thanks go to S. Pinkerneil of the GFZ for sample preparation and elemental and stable isotope measurements. We thank two anonymous reviewers, who provided very informative comments, and thus helped to improve the quality of the article. We gratefully acknowledge the cooperation by the Forest and Wildlife Department of Maharashtra State, India. Funding was provided by the German Research Foundation (Grants: GA 755/7-1; PR 755/7-2) within the framework of the project "Himalaya: Modern and Past Climates" (HIMPAC; FOR 1380).

References

Agnihotri, R., Kurian, S., Fernandes, M., Reshma, K., D'Souza, W., Naqvi, S.W.A., 2008. Variability of subsurface denitrification and surface productivity in the coastal eastern Arabian Sea over the past seven centuries. The Holocene 18, 755–764. http://dx.doi.org/10.1177/0959683608091795.

Alizai, A., Hillier, S., Clift, P.D., Giosan, L., Hurst, A., VanLaningham, S., Macklin, M., 2012. Clay mineral variations in Holocene terrestrial sediments from the Indus Basin. Quat. Res. 77, 368–381. http://dx.doi.org/10.1016/j.yqres.2012.01.008.

Alley, R.B., Mayewski, P.A., Sowers, T., Stuiver, M., Taylor, K.C., Clark, P.U., 1997. Holocene climatic instability: a prominent, widespread event 8200 yr ago. Geology 25, 483–486. http://dx.doi.org/10.1130/0091-7613(1997)025<0483:hciapw>2.3.co;2.

Amundson, R., Austin, A.T., Schuur, E.A.G., Yoo, K., Matzek, V., Kendall, C., Uebersax, A., Brenner, D., Baisden, W.T., 2003. Global patterns of the isotopic composition of soil and plant nitrogen. Glob. Biogeochem. Cycles 17, 1031. http://dx.doi.org/10.1029/2002gb001903.

Anderson, D.M., Overpeck, J.T., Gupta, A.K., 2002. Increase in the Asian southwest monsoon during the past four centuries. Science 297, 596–599. http://dx.doi.org/10.1126/science.1072881.

Anoop, A., Prasad, S., Krishnan, R., Naumann, R., Dulski, P., 2013a. Intensified monsoon and spatiotemporal changes in precipitation patterns in the NW Himalaya during the early-mid Holocene. Quat. Int. 313–314, 74–84. http://dx.doi.org/10.1016/j.quaint.2013.08.014.

Anoop, A., Prasad, S., Plessen, B., Basavaiah, N., Gaye, B., Naumann, R., Menzel, P., Weise, S., Brauer, A., 2013b. Palaeoenvironmental implications of evaporative gaylussite crystals from Lonar Lake, central India. J. Quat. Sci. 28, 349–359. http://dx.doi.org/10.1002/jqs.2625.

Badve, R.M., Kumaran, K.P.N., Rajshekhar, C., 1993. Eutrophication of Lonar Lake, Maharashtra. Curr. Sci. 65, 347–351.

Bamzai, A.S., Shukla, J., 1999. Relation between Eurasian snow cover, snow depth, and the Indian summer monsoon: an observational study. J. Clim. 12, 3117–3132. http://dx.doi.org/10.1175/1520-0442(1999)012<3117:rbescs>2.0.co;2.

Barber, D.C., Dyke, A., Hillaire-Marcel, C., Jennings, A.E., Andrews, J.T., Kerwin, M.W., Bilodeau, G., McNeely, R., Southon, J., Morehead, M.D., Gagnon, J.M., 1999. Forcing of the cold event of 8,200 years ago by catastrophic drainage of Laurentide lakes. Nature 400, 344–348. http://dx.doi.org/10.1038/22504.

Bar-Matthews, M., Ayalon, A., Kaufman, A., 1997. Late Quaternary paleoclimate in the eastern Mediterranean region from stable isotope analysis of speleothems at Soreq Cave, Israel. Quat. Res. 47, 155–168. http://dx.doi.org/10.1006/qres.1997.1883.

Barnett, T.P., Dümenil, L., Schlese, U., Roeckner, E., Latif, M., 1989. The effect of Eurasian snow cover on regional and global climate variations. J. Atmos. Sci. 46, 661–685. http://dx.doi.org/10.1175/1520-0469(1989)046<0661:teoesc>2.0.co;2.

Basavaiah, N., Wiesner, M.G., Anoop, A., Menzel, P., Nowaczyk, N.R., Deenadayalan, K., Brauer, A., Gaye, B., Naumann, R., Riedel, N., Prasad, M.S.S., 2014. Physicochemical analyses of surface sediments from the Lonar Lake, central India — implications for palaeoenvironmental reconstruction. Fundam. Appl. Limnol. 184, 51–68. http://dx.doi.org/10.1127/1863-9135/2010/0515.

Beer, J., 2000. Long-term indirect indices of solar variability. Space Sci. Rev. 94, 53–66. http://dx.doi.org/10.1023/a:1026778013901.

Berger, A., Loutre, M.F., 1991. Insolation values for the climate of the last 10 million years. Quat. Sci. Rev. 10, 297–317. http://dx.doi.org/10.1016/0277-3791(91)90033-q.

Berkelhammer, M., Sinha, A., Mudelsee, M., Cheng, H., Edwards, R.L., Cannariato, K., 2010. Persistent multidecadal power of the Indian Summer Monsoon. Earth Planet. Sci. Lett. 290, 166–172. http://dx.doi.org/10.1016/j.epsl.2009.12.017.

Bond, G., Showers, W., Cheseby, M., Lotti, R., Almasi, P., deMenocal, P., Priore, P., Cullen, H., Hajdas, I., Bonani, G., 1997. A pervasive millennial-scale cycle in North Atlantic Holocene and glacial climates. Science 278, 1257–1266. http://dx.doi.org/10.1126/science.278.5341.1257.

Bond, G., Kromer, B., Beer, J., Muscheler, R., Evans, M.N., Showers, W., Hoffmann, S., Lotti-Bond, R., Hajdas, I., Bonani, G., 2001. Persistent solar influence on North Atlantic climate during the Holocene. Science 294, 2130–2136. http://dx.doi.org/10.1126/science.1065680.

Bookhagen, B., Thiede, R.C., Strecker, M.R., 2005. Late Quaternary intensified monsoon phases control landscape evolution in the northwest Himalaya. Geology 33, 149–152. http://dx.doi.org/10.1130/g20982.1.

Broccoli, A.J., Dahl, K.A., Stouffer, R.J., 2006. Response of the ITCZ to Northern Hemisphere cooling. Geophys. Res. Lett. 33, L01702. http://dx.doi.org/10.1029/2005gl024546.

Bronk Ramsey, C., 2008. Deposition models for chronological records. Quat. Sci. Rev. 27, 42–60. http://dx.doi.org/10.1016/j.quascirev.2007.01.019.

Caner, L., Lo Seen, D., Gunnell, Y., Ramesh, B.R., Bourgeon, G., 2007. Spatial heterogeneity of land cover response to climatic change in the Nilgiri highlands (Southern India) since the last glacial maximum. The Holocene 17, 195–205. http://dx.doi.org/10.1177/0959683607075833.

Casciotti, K.L., Buchwald, C., Santoro, A.E., Frame, C., 2011. Assessment of nitrogen and oxygen isotopic fractionation during nitrification and its expression in the marine environment. In: Klotz, M.G. (Ed.), Methods in Enzymology: Research on Nitrification and Related Processes, Vol 486, Part A. vol. 486. Elsevier Academic Press Inc., San Diego, pp. 253–280. http://dx.doi.org/10.1016/B978-0-12-381294-0.00011-0.

Clift, P.D., Giosan, L., Blusztajn, J., Campbell, I.H., Allen, C., Pringle, M., Tabrez, A.R., Danish, M., Rabbani, M.M., Alizai, A., Carter, A., Lückge, A., 2008. Holocene erosion of the Lesser Himalaya triggered by intensified summer monsoon. Geology 36, 79–82. http://dx.doi.org/10.1130/g24315a.1.

Clift, P.D., Carter, A., Giosan, L., Durcan, J., Duller, G.A.T., Macklin, M.G., Alizai, A., Tabrez, A.R., Danish, M., VanLaningham, S., Fuller, D.Q., 2012. U–Pb zircon dating evidence for a Pleistocene Sarasvati River and capture of the Yamuna River. Geology 40, 211–214. http://dx.doi.org/10.1130/g32840.1.

Cowie, G.L., Hedges, J.I., Prahl, F.G., de Lange, G.J., 1995. Elemental and major biochemical changes across an oxidation front in a relict turbidite: an oxygen effect. Geochim. Cosmochim. Acta 59, 33–46. http://dx.doi.org/10.1016/0016-7037(94)00329-k.

Dauwe, B., Middelburg, J.J., 1998. Amino acids and hexosamines as indicators of organic matter degradation state in North Sea sediments. Limnol. Oceanogr. 43, 782–798. http://dx.doi.org/10.4319/lo.1998.43.5.0782.

Dauwe, B., Middelburg, J.J., Herman, P.M.J., Heip, C.H.R., 1999. Linking diagenetic alteration of amino acids and bulk organic matter reactivity. Limnol. Oceanogr. 44, 1809–1814. http://dx.doi.org/10.4319/lo.1999.44.7.1809.

Demske, D., Tarasov, P.E., Wünnemann, B., Riedel, F., 2009. Late glacial and Holocene vegetation, Indian monsoon and westerly circulation in the Trans-Himalaya recorded in the lacustrine pollen sequence from Tso Kar, Ladakh, NW India. Palaeogeogr. Palaeoclimatol. Palaeoecol. 279, 172–185. http://dx.doi.org/10.1016/j.palaeo.2009.05.008.

Denniston, R.F., González, L.A., Asmerom, Y., Sharma, R.H., Reagan, M.K., 2000. Speleothem evidence for changes in Indian summer monsoon precipitation over the last ~2300 years. Quat. Res. 53, 196–202. http://dx.doi.org/10.1006/qres.1999.2111.

Dykoski, C.A., Edwards, R.L., Cheng, H., Yuan, D.X., Cai, Y.J., Zhang, M.L., Lin, Y.S., Qing, J.M., An, Z.S., Revenaugh, J., 2005. A high-resolution, absolute-dated Holocene and deglacial Asian monsoon record from Dongge Cave, China. Earth Planet. Sci. Lett. 233, 71–86. http://dx.doi.org/10.1016/j.epsl.2005.01.036.

Enzel, Y., Ely, L.L., Mishra, S., Ramesh, R., Amit, R., Lazar, B., Rajaguru, S.N., Baker, V.R., Sandler, A., 1999. High-resolution Holocene environmental changes in the Thar Desert, northwestern India. Science 284, 125–128. http://dx.doi.org/10.1126/science.284.5411.125.

Fleitmann, D., Burns, S.J., Mangini, A., Mudelsee, M., Kramers, J., Villa, I., Neff, U., Al-Subbary, A.A., Buettner, A., Hippler, D., Matter, A., 2007. Holocene ITCZ and Indian monsoon dynamics recorded in stalagmites from Oman and Yemen (Socotra). Quat. Sci. Rev. 26, 170–188. http://dx.doi.org/10.1016/j.quascirev.2006.04.012.

Fleitmann, D., Mudelsee, M., Burns, S.J., Bradley, R.S., Kramers, J., Matter, A., 2008. Evidence for a widespread climatic anomaly at around 9.2 ka before present. Paleoceanography 23. http://dx.doi.org/10.1029/2007pa001519.

Freudenthal, T., Wagner, T., Wenzhöfer, F., Zabel, M., Wefer, G., 2001. Early diagenesis of organic matter from sediments of the eastern subtropical Atlantic: evidence from stable nitrogen and carbon isotopes. Geochim. Cosmochim. Acta 65, 1795–1808. http://dx.doi.org/10.1016/s0016-7037(01)00554-3.

Gadgil, S., 2003. The Indian monsoon and its variability. Annu. Rev. Earth Planet. Sci. 31, 429–467. http://dx.doi.org/10.1146/annurev.earth.31.100901.141251.

Gasse, F., 2000. Hydrological changes in the African tropics since the Last Glacial Maximum. Quat. Sci. Rev. 19, 189–211. http://dx.doi.org/10.1016/s0277-3791(99)00061-x.

Gasse, F., Arnold, M., Fontes, J.-C., Fort, M., Gibert, E., Huc, A., Li, B.Y., Li, Y.F., Liu, Q., Mélières, F., Van Campo, E., Wang, F.B., Zhang, Q.S., 1991. A 13.000-year climate record from western Tibet. Nature 353, 742–745. http://dx.doi.org/10.1038/353742a0.

Gasse, F., Fontes, J.-C., Van Campo, E., Wei, K., 1996. Holocene environmental changes in Bangong Co basin (Western Tibet). Part 4: discussion and conclusions. Palaeogeogr. Palaeoclimatol. Palaeoecol. 120, 79–92. http://dx.doi.org/10.1016/0031-0182(95)00035-6.

Giosan, L., Clift, P.D., Macklin, M.G., Fuller, D.Q., Constantinescu, S., Durcan, J.A., Stevens, T., Duller, G.A.T., Tabrez, A.R., Gangal, K., Adhikari, R., Alizai, A., Filip, F., VanLaningham, S., Syvitski, J.P.M., 2012. Fluvial landscapes of the Harappan civilization. Proc. Natl. Acad. Sci. 109, E1688–E1694. http://dx.doi.org/10.1073/pnas.1112743109.

Gu, B.H., Schelske, C.L., Hodell, D.A., 2004. Extreme ^{13}C enrichments in a shallow hypereutrophic lake: implications for carbon cycling. Limnol. Oceanogr. 49, 1152–1159. http://dx.doi.org/10.4319/lo.2004.49.4.1152.

Gupta, A.K., Anderson, D.M., Overpeck, J.T., 2003. Abrupt changes in the Asian southwest monsoon during the Holocene and their links to the North Atlantic Ocean. Nature 421, 354–357. http://dx.doi.org/10.1038/nature01340.

Gupta, A.K., Das, M., Anderson, D.M., 2005. Solar influence on the Indian summer monsoon during the Holocene. Geophys. Res. Lett. 32. http://dx.doi.org/10.1029/2005gl022685.

Gupta, A.K., Anderson, D.M., Pandey, D.N., Singhvi, A.K., 2006. Adaptation and human migration, and evidence of agriculture coincident with changes in the Indian summer monsoon during the Holocene. Curr. Sci. 90, 1082–1090.

Haug, G.H., Hughen, K.A., Sigman, D.M., Peterson, L.C., Röhl, U., 2001. Southward migration of the intertropical convergence zone through the Holocene. Science 293, 1304–1308. http://dx.doi.org/10.1126/science.1059725.

Hodell, D.A., Schelske, C.L., 1998. Production, sedimentation, and isotopic composition of organic matter in Lake Ontario. Limnol. Oceanogr. 43, 200–214. http://dx.doi.org/10.4319/lo.1998.43.2.0200.

Hodell, D.A., Brenner, M., Kanfoush, S.L., Curtis, J.H., Stoner, J.S., Song, X.L., Wu, Y., Whitmore, T.J., 1999. Paleoclimate of Southwestern China for the past 50,000 yr inferred from lake sediment records. Quat. Res. 52, 369–380. http://dx.doi.org/10.1006/qres.1999.2072.

Hong, Y.T., Hong, B., Lin, Q.H., Zhu, Y.X., Shibata, Y., Hirota, M., Uchida, M., Leng, X.T., Jiang, H.B., Xu, H., Wang, H., Yi, L., 2003. Correlation between Indian Ocean summer monsoon and North Atlantic climate during the Holocene. Earth Planet. Sci. Lett. 211, 371–380. http://dx.doi.org/10.1016/s0012-821x(03)00207-3.

Johnsen, S.J., Dahl-Jensen, D., Gundestrup, N., Steffensen, J.P., Clausen, H.B., Miller, H., Masson-Delmotte, V., Sveinbjörnsdottir, A.E., White, J., 2001. Oxygen isotope and palaeotemperature records from six Greenland ice-core stations: Camp Century, Dye-3, GRIP, GISP2, Renland and NorthGRIP. J. Quat. Sci. 16, 299–307. http://dx.doi.org/10.1002/jqs.622.

Joshi, A.A., Kanekar, P.P., Kelkar, A.S., Shouche, Y.S., Vani, A.A., Borgave, S.B., Sarnaik, S.S., 2008. Cultivable bacterial diversity of alkaline Lonar Lake, India. Microb. Ecol. 55, 163–172. http://dx.doi.org/10.1007/s00248-007-9264-8.

Jourdan, F., Moynier, F., Koeberl, C., Eroglu, S., 2011. $^{40}Ar/^{39}Ar$ age of the Lonar crater and consequence for the geochronology of planetary impacts. Geology 39, 671–674. http://dx.doi.org/10.1130/g31888.1.

Kauppila, T., Salonen, V.-P., 1997. The effect of Holocene treeline fluctuations on the sediment chemistry of Lake Kilpisjärvi, Finland. J. Paleolimnol. 18, 145–163. http://dx.doi.org/10.1023/a:1007978318562.

Kendall, R.A., Mitrovica, J.X., Milne, G.A., Törnqvist, T.E., Li, Y.X., 2008. The sea-level fingerprint of the 8.2 ka climate event. Geology 36, 423–426. http://dx.doi.org/10.1130/G24550A.1.

Kennett, D.J., Breitenbach, S.F.M., Aquino, V.V., Asmerom, Y., Awe, J., Baldini, J.U.L., Bartlein, P., Culleton, B.J., Ebert, C., Jazwa, C., Macri, M.J., Marwan, N., Polyak, V., Prufer, K.M., Ridley, H.E., Sodemann, H., Winterhalder, B., Haug, G.H., 2012. Development and disintegration of Maya political systems in response to climate change. Science 338, 788–791. http://dx.doi.org/10.1126/science.1226299.

Koinig, K., Shotyk, W., Lotter, A., Ohlendorf, C., Sturm, M., 2003. 9000 years of geochemical evolution of lithogenic major and trace elements in the sediment of an alpine lake — the role of climate, vegetation, and land-use history. J. Paleolimnol. 30, 307–320. http://dx.doi.org/10.1023/a:1026080712312.

Koutavas, A., Sachs, J.P., 2008. Northern timing of deglaciation in the eastern equatorial Pacific from alkenone paleothermometry. Paleoceanography 23, PA4205. http://dx.doi.org/10.1029/2008pa001593.

Lahajnar, N., Wiesner, M.G., Gaye, B., 2007. Fluxes of amino acids and hexosamines to the deep South China Sea. Deep-Sea Res. I 54, 2120–2144. http://dx.doi.org/10.1016/j.dsr.2007.08.009.

Lehmann, M.F., Bernasconi, S.M., Barbieri, A., McKenzie, J.A., 2002. Preservation of organic matter and alteration of its carbon and nitrogen isotope composition during simulated and in situ early sedimentary diagenesis. Geochim. Cosmochim. Acta 66, 3573–3584. http://dx.doi.org/10.1016/S0016-7037(02)00968-7.

Lehmann, M.F., Bernasconi, S.M., McKenzie, J.A., Barbieri, A., Simona, M., Veronesi, M., 2004. Seasonal variation of the $\delta^{13}C$ and $\delta^{15}N$ of particulate and dissolved carbon and nitrogen in Lake Lugano: Constraints on biogeochemical cycling in a eutrophic lake. Limnol. Oceanogr. 49, 415–429. http://dx.doi.org/10.4319/lo.2004.49.2.0415.

Lei, Y.B., Yao, T.D., Sheng, Y.W., Zhang, E.L., Wang, W.C., Li, J.L., 2012. Characteristics of $\delta^{13}C_{DIC}$ in lakes on the Tibetan Plateau and its implications for the carbon cycle. Hydrol. Process. 26, 535–543. http://dx.doi.org/10.1002/hyp.8152.

Liu, Y.H., Henderson, G.M., Hu, C.Y., Mason, A.J., Charnley, N., Johnson, K.R., Xie, S.C., 2013. Links between the East Asian monsoon and North Atlantic climate during the 8,200 year event. Nat. Geosci. 6, 117–120. http://dx.doi.org/10.1038/ngeo1708.

Loutre, M.F., Berger, A., Bretagnon, P., Blanca, P.L., 1992. Astronomical frequencies for climate research at the decadal to century time scale. Clim. Dyn. 7, 181–194. http://dx.doi.org/10.1007/bf00206860.

MacDonald, G., 2011. Potential influence of the Pacific Ocean on the Indian summer monsoon and Harappan decline. Quat. Int. 229, 140–148. http://dx.doi.org/10.1016/j.quaint.2009.11.012.

Madella, M., Fuller, D.Q., 2006. Palaeoecology and the Harappan Civilisation of South Asia: a reconsideration. Quat. Sci. Rev. 25, 1283–1301. http://dx.doi.org/10.1016/j.quascirev.2005.10.012.

Magny, M., Joannin, S., Galop, D., Vannière, B., Haas, J.N., Bassetti, M., Bellintani, P., Scandolari, R., Desmet, M., 2012. Holocene palaeohydrological changes in the northern Mediterranean borderlands as reflected by the lake-level record of Lake Ledro, northeastern Italy. Quat. Res. 77, 382–396. http://dx.doi.org/10.1016/j.yqres.2012.01.005.

Mahajan, A.D., 2005. Preliminary survey of planktonic diversity in Lonar lake water. In: Banmeru, P.K., Banmeru, S.K., Mishra, V.R. (Eds.), Biodiversity of Lonar Crater. Anamaya Publishers, New Delhi, India, pp. 58–62.

Malu, R.A., Kulkarni, K.M., Kodarkar, M.S., 2005. Conservation and management of biotic environment in Lonar crater lake: an ecological wonder of India. In: Banmeru, P.K., Banmeru, S.K., Mishra, V.R. (Eds.), Biodiversity of Lonar Crater. Anamaya Publishers, New Delhi, pp. 39–46.

Mayewski, P.A., Rohling, E.E., Stager, J.C., Karlén, W., Maasch, K.A., Meeker, L.D., Meyerson, E.A., Gasse, F., van Kreveld, S., Holmgren, K., Lee-Thorp, J., Rosqvist, G., Rack, F., Staubwasser, M., Schneider, R.R., Steig, E.J., 2004. Holocene climate variability. Quat. Res. 62, 243–255. http://dx.doi.org/10.1016/j.yqres.2004.07.001.

McLaren, P., Bowles, D., 1985. The effects of sediment transport on grain-size distributions. J. Sediment. Res. 55, 457–470. http://dx.doi.org/10.1306/212f86fc-2b24-11d7-8648000102c1865d.

Mengel, K., 1996. Turnover of organic nitrogen in soils and its availability to crops. Plant Soil 181, 83–93. http://dx.doi.org/10.1007/bf00011295.

Menzel, P., Gaye, B., Wiesner, M.G., Prasad, S., Stebich, M., Das, B.K., Anoop, A., Riedel, N., Basavaiah, N., 2013. Influence of bottom water anoxia on nitrogen isotopic ratios and amino acid contributions of recent sediments from small eutrophic Lonar Lake, central India. Limnol. Oceanogr. 58, 1061–1074. http://dx.doi.org/10.4319/lo.2013.58.3.1061.

Meyers, P.A., 1997. Organic geochemical proxies of paleoceanographic, paleolimnologic, and paleoclimatic processes. Org. Geochem. 27, 213–250. http://dx.doi.org/10.1016/S0146-6380(97)00049-1.

Meyers, P.A., Ishiwatari, R., 1993. Lacustrine organic geochemistry: an overview of indicators of organic matter sources and diagenesis in lake sediments. Org. Geochem. 20, 867–900. http://dx.doi.org/10.1016/0146-6380(93)90100-P.

Meyers, P.A., Lallier-Vergès, E., 1999. Lacustrine sedimentary organic matter records of Late Quaternary paleoclimates. J. Paleolimnol. 21, 345–372. http://dx.doi.org/10.1023/a:1008073732192.

Morrill, C., Overpeck, J.T., Cole, J.E., 2003. A synthesis of abrupt changes in the Asian summer monsoon since the last deglaciation. The Holocene 13, 465–476. http://dx.doi.org/10.1191/0959683603hl639ft.

Moy, C.M., Seltzer, G.O., Rodbell, D.T., Anderson, D.M., 2002. Variability of El Nino/Southern Oscillation activity at millennial timescales during the Holocene epoch. Nature 420, 162–165. http://dx.doi.org/10.1038/nature01194.

Nandy, N.C., Deo, V.B., 1961. Origin of the Lonar Lake and its alkalinity. Tech. J. Tata Iron Steel Co. 8, 144–155.

O'Leary, M.H., 1988. Carbon isotopes in photosynthesis. Bioscience 38, 328–336. http://dx.doi.org/10.2307/1310735.

Overpeck, J.T., Anderson, D.M., Trumbore, S., Prell, W.L., 1996. The southwest Indian Monsoon over the last 18000 years. Clim. Dyn. 12, 213–225. http://dx.doi.org/10.1007/bf00211619.

Parker, A.G., Eckersley, L., Smith, M.M., Goudie, A.S., Stokes, S., Ward, S., White, K., Hodson, M.J., 2004. Holocene vegetation dynamics in the northeastern Rub' al-Khali desert, Arabian Peninsula: a phytolith, pollen and carbon isotope study. J. Quat. Sci. 19, 665–676. http://dx.doi.org/10.1002/jqs.880.

Pausata, F.S.R., Battisti, D.S., Nisancioglu, K.H., Bitz, C.M., 2011. Chinese stalagmite $\delta^{18}O$ controlled by changes in the Indian monsoon during a simulated Heinrich event. Nat. Geosci. 4, 474–480. http://dx.doi.org/10.1038/ngeo1169.

Peng, Y., Xiao, J., Nakamura, T., Liu, B., Inouchi, Y., 2005. Holocene East Asian monsoonal precipitation pattern revealed by grain-size distribution of core sediments of Daihai Lake in Inner Mongolia of north-central China. Earth Planet. Sci. Lett. 233, 467–479. http://dx.doi.org/10.1016/j.epsl.2005.02.022.

Peterson, B.J., Fry, B., 1987. Stable isotopes in ecosystem studies. Annu. Rev. Ecol. Syst. 18, 293–320. http://dx.doi.org/10.1146/annurev.es.18.110187.001453.

Possehl, G.L., 1997. The transformation of the Indus Civilization. J. World Prehist. 11, 425–472. http://dx.doi.org/10.1007/bf02220556.

Prasad, S., Enzel, Y., 2006. Holocene paleoclimates of India. Quat. Res. 66, 442–453. http://dx.doi.org/10.1016/j.yqres.2006.05.008.

Prasad, S., Anoop, A., Riedel, N., Sarkar, S., Menzel, P., Basavaiah, N., Krishnan, R., Fuller, D. Q., Plessen, B., Gaye, B., Röhl, U., Wilkes, H., Sachse, D., Sawant, R., Wiesner, M.G., Stebich, M., 2014. Prolonged monsoon droughts and links to Indo-Pacific warm pool: a Holocene record from Lonar Lake, central India. Earth Planet. Sci. Lett. 391, 171–182. http://dx.doi.org/10.1016/j.epsl.2014.01.043.

Prasad, V., Farooqui, A., Sharma, A., Phartiyal, B., Chakraborty, S., Bhandari, S., Raj, R., Singh, A., 2014. Mid–late Holocene monsoonal variations from mainland Gujarat, India: a multiproxy study for evaluating climate culture relationship. Palaeogeogr. Palaeoclimatol. Palaeoecol. 397, 38–51. http://dx.doi.org/10.1016/j.palaeo.2013.05.025.

Rehfeld, K., Marwan, N., Heitzig, J., Kurths, J., 2011. Comparison of correlation analysis techniques for irregularly sampled time series. Nonlinear Process. Geophys. 18, 389–404. http://dx.doi.org/10.5194/npg-18-389-2011.

Rein, B., Lückge, A., Reinhardt, L., Sirocko, F., Wolf, A., Dullo, W.C., 2005. El Niño variability off Peru during the last 20,000 years. Paleoceanography 20. http://dx.doi.org/10.1029/2004pa001099.

Roth, M., Hampa , A., 1973. Column chromatography of amino acids with fluorescence detection. J. Chromatogr. A 83, 353–356. http://dx.doi.org/10.1016/S0021-9673(00)97051-1.

Sharma, S., Joachimski, M., Sharma, M., Tobschall, H.J., Singh, I.B., Sharma, C., Chauhan, M. S., Morgenroth, G., 2004. Lateglacial and Holocene environmental changes in Ganga plain, Northern India. Quat. Sci. Rev. 23, 145–159. http://dx.doi.org/10.1016/j.quascirev.2003.10.005.

Singh, G., 1971. The Indus Valley culture: seen in the context of post-glacial climatic and ecological studies in north-west India. Archaeol. Phys. Anthropol. Ocean. 6, 177–189.

Sinha, A., Cannariato, K.G., Stott, L.D., Cheng, H., Edwards, R.L., Yadava, M.G., Ramesh, R., Singh, I.B., 2007. A 900-year (600 to 1500 A.D.) record of the Indian summer monsoon precipitation from the core monsoon zone of India. Geophys. Res. Lett. 34. http://dx.doi.org/10.1029/2007gl030431.

Sollins, P., Spycher, G., Glassman, C.A., 1984. Net nitrogen mineralization from light- and heavy-fraction forest soil organic matter. Soil Biol. Biochem. 16, 31–37. http://dx.doi.org/10.1016/0038-0717(84)90122-6.

Soon, W., Velasco Herrera, V.M., Selvaraj, K., Traversi, R., Usoskin, I., Chen, C.-T.A., Lou, J.-Y., Kao, S.-J., Carter, R.M., Pipin, V., Severi, M., Becagli, S., 2014. A review of Holocene solar-linked climatic variation on centennial to millennial timescales: physical processes, interpretative frameworks and a new multiple cross-wavelet transform algorithm. Earth Sci. Rev. 134, 1–15. http://dx.doi.org/10.1016/j.earscirev.2014.03.003.

Staubwasser, M., Weiss, H., 2006. Holocene climate and cultural evolution in late prehistoric–early historic West Asia. Quat. Res. 66, 372–387. http://dx.doi.org/10.1016/j.yqres.2006.09.001.

Stuiver, M., 1975. Climate versus changes in ^{13}C content of the organic component of lake sediments during the Late Quaternary. Quat. Res. 5, 251–262. http://dx.doi.org/10.1016/0033-5894(75)90027-7.

Stuiver, M., Grootes, P.M., 2000. GISP2 oxygen isotope ratios. Quat. Res. 53, 277–284. http://dx.doi.org/10.1006/qres.2000.2127.

Sun, D., Bloemendal, J., Rea, D.K., Vandenberghe, J., Jiang, F., An, Z., Su, R., 2002. Grain-size distribution function of polymodal sediments in hydraulic and aeolian environments, and numerical partitioning of the sedimentary components. Sediment. Geol. 152, 263–277. http://dx.doi.org/10.1016/S0037-0738(02)00082-9.

Surakasi, V.P., Wani, A.A., Shouche, Y.S., Ranade, D.R., 2007. Phylogenetic analysis of methanogenic enrichment cultures obtained from Lonar Lake in India: isolation of *Methanocalculus* sp. and *Methanoculleus* sp. Microb. Ecol. 54, 697–704. http://dx.doi.org/10.1007/s00248-007-9228-z.

Talbot, M.R., Lærdal, T., 2000. The Late Pleistocene–Holocene palaeolimnology of Lake Victoria, East Africa, based upon elemental and isotopic analyses of sedimentary organic matter. J. Paleolimnol. 23, 141–164. http://dx.doi.org/10.1023/a:1008029400463.

Teller, J.T., Leverington, D.W., Mann, J.D., 2002. Freshwater outbursts to the oceans from glacial Lake Agassiz and their role in climate change during the last deglaciation. Quat. Sci. Rev. 21, 879–887. http://dx.doi.org/10.1016/S0277-3791(01)00145-7.

Thompson, L.G., Yao, T., Mosley-Thompson, E., Davis, M.E., Henderson, K.A., Lin, P.-N., 2000. A high-resolution millennial record of the South Asian Monsoon from Himalayan ice cores. Science 289, 1916–1919. http://dx.doi.org/10.1126/science.289.5486.1916.

Tieszen, L.L., Senyimba, M.M., Imbamba, S.K., Troughton, J.H., 1979. The distribution of C_3 and C_4 grasses and carbon isotope discrimination along an altitudinal and moisture gradient in Kenya. Oecologia 37, 337–350.

Tripathi, J.K., Bock, B., Rajamani, V., Eisenhauer, A., 2004. Is River Ghaggar, Saraswati? Geochemical constraints. Curr. Sci. 87, 1141–1145.

Wang, Y.J., Cheng, H., Edwards, R.L., An, Z.S., Wu, J.Y., Shen, C.-C., Dorale, J.A., 2001. A high-resolution absolute-dated Late Pleistocene monsoon record from Hulu Cave, China. Science 294, 2345–2348. http://dx.doi.org/10.1126/science.1064618.

Wang, Y.J., Cheng, H., Edwards, R.L., He, Y.Q., Kong, X.G., An, Z.S., Wu, J.Y., Kelly, M.J., Dykoski, C.A., Li, X.D., 2005. The Holocene Asian monsoon: links to solar changes and North Atlantic climate. Science 308, 854–857. http://dx.doi.org/10.1126/science.1106296.

Wei, K., Gasse, F., 1999. Oxygen isotopes in lacustrine carbonates of West China revisited: implications for post glacial changes in summer monsoon circulation. Quat. Sci. Rev. 18, 1315–1334. http://dx.doi.org/10.1016/s0277-3791(98)00115-2.

Wilmshurst, J.M., 1997. The impact of human settlement on vegetation and soil stability in Hawke's Bay, New Zealand. N. Z. J. Bot. 35, 97–111. http://dx.doi.org/10.1080/0028825x.1997.10410672.

Wünnemann, B., Demske, D., Tarasov, P., Kotlia, B.S., Reinhardt, C., Bloemendal, J., Diekmann, B., Hartmann, K., Krois, J., Riedel, F., Arya, N., 2010. Hydrological evolution during the last 15 kyr in the Tso Kar lake basin (Ladakh, India), derived from geomorphological, sedimentological and palynological records. Quat. Sci. Rev. 29, 1138–1155. http://dx.doi.org/10.1016/j.quascirev.2010.02.017.

Yadava, M.G., Ramesh, R., 2005. Monsoon reconstruction from radiocarbon dated tropical Indian speleothems. The Holocene 15, 48–59. http://dx.doi.org/10.1191/0959683605h1783rp.

Zhang, J., Quay, P.D., Wilbur, D.O., 1995. Carbon isotope fractionation during gas–water exchange and dissolution of CO_2. Geochim. Cosmochim. Acta 59, 107–114. http://dx.doi.org/10.1016/0016-7037(95)91550-d.